Integrated Ocean Drilling Program
Expeditions 304 and 305 Scientific Prospectus

Oceanic Core Complex Formation, Atlantis Massif

Oceanic core complex formation, Atlantis Massif, Mid-Atlantic Ridge: drilling into the footwall and hanging wall of a tectonic exposure of deep, young oceanic lithosphere to study deformation, alteration, and melt generation

Dr. Donna K. Blackman
Co-Chief Scientist
Scripps Institution of Oceanography
University of California, San Diego
9500 Gilman Drive
La Jolla CA 92093-0225
USA

Dr. Barbara E. John
Co-Chief Scientist
Department of Geology and Geophysics
1000 University Avenue
University of Wyoming
Laramie WY 82071
USA

Dr. Benoit Ildefonse
Co-Chief Scientist
Laboratoire de Tectonophysique
Universite Montpellier II
Universite Montpellier 2, CC49
34095 Montpellier
France

Dr. Yasuhiko Ohara
Co-Chief Scientist
Ocean Research Laboratory
Hydrographic and Oceanographic
Department of Japan
5-3-1 Tsukiji, Chuo-ku
Tokyo 104-0045
Japan

Dr. Christopher J. MacLeod
Co-Chief Scientist
Department of Earth Sciences
Cardiff University
Main College, Park Place
Cardiff, Wales CF10 3YE
United Kingdom

Dr. D. Jay Miller
Expedition Project Manager and Staff Scientist
Integrated Ocean Drilling Program
Texas A&M University
1000 Discovery Drive
College Station TX 77845-9547
USA

August 2004

PUBLISHER'S NOTES

Citation:
Blackman, D.K., Ildefonse, B., John, B.E., MacLeod, C.J., Ohara, Y., Miller, D.J., and the Expedition 304/305 Project Team, 2004. Oceanic core complex formation, Atlantis Massif—oceanic core complex formation, Atlantis Massif, Mid-Atlantic Ridge: drilling into the footwall and hanging wall of a tectonic exposure of deep, young oceanic lithosphere to study deformation, alteration, and melt generation. *IODP Sci. Prosp.,* 304/305. http://iodp.tamu.edu/publications/SP/304305SP/304305SP.PDF.

Distribution:
Electronic copies of this series may be obtained from the Integrated Ocean Drilling Program (IODP) Publication Services homepage on the World Wide Web at **iodp.tamu.edu/publications.**

This publication was prepared by the Integrated Ocean Drilling Program U.S. Implementing Organization (IODP-USIO): Joint Oceanographic Institutions, Inc., Lamont Doherty Earth Observatory of Columbia University, and Texas A&M University (TAMU), as an account of work performed under the international Integrated Ocean Drilling Program, which is managed by IODP Management International (IODP-MI), Inc. Funding for the program is provided by the following agencies:

European Consortium for Ocean Research Drilling (ECORD)

Ministry of Education, Culture, Sports, Science and Technology (MEXT) of Japan

Ministry of Science and Technology (MOST), People's Republic of China

U.S. National Science Foundation (NSF)

DISCLAIMER

This IODP Scientific Prospectus is based on precruise Science Advisory Structure panel discussions and scientific input from the designated Co-Chief Scientists on behalf of the drilling proponents. During the course of the cruise, actual site operations may indicate to the Co-Chief Scientists and the Operations Superintendent that it would be scientifically or operationally advantageous to amend the plan detailed in this prospectus. It should be understood that any proposed changes to the science deliverables outlined in the plan presented here are contingent upon the approval of the IODP-USIO Science Services, TAMU, Deputy Director of Science Services in consultation with IODP-MI.

ABSTRACT

Atlantis Massif exposes serpentinized peridotite and lesser gabbro in a domal high at the inside corner of the eastern intersection of the Mid-Atlantic Ridge (MAR) at 30°N and the Atlantis Fracture Zone. The goals for Integrated Ocean Drilling Program (IODP) drilling during Expeditions 304 and 305 are to characterize variations in rock type, structure, and alteration with depth at this ultramafic oceanic core complex and to obtain core of essentially fresh, in situ peridotite. Drilling, coring, and wireline logging will document the composition, microstructure, and evidence for melt production/migration and the relationships between these factors, as well as syntectonic alteration. This study of lithospheric formation and the causes of variation in crustal structure at slow-spreading centers addresses the Solid Earth Cycles and Geodynamics portion of the IODP Initial Science Plan.

Domal massifs capped by corrugated detachment faults have been mapped at several locations on the seafloor. Formation of these large, shallow seafloor features appears to be an episodic manifestation of plate rifting and accretion at slow-spreading ridges. At Atlantis Massif we have the opportunity to core and log the detachment zone at both exposed (footwall) and unexposed (beneath the adjacent hanging wall) sites to address the characteristics of strain localization and the effects of fluid flow. Genetic relationships between the geochemistry of hanging wall basalt and footwall lithologies will be studied, as will patterns of block rotation within and between the footwall and the hanging wall.

At the footwall site, the nature of an alteration front within oceanic lithosphere will be studied. Seawater alteration profoundly affects the geophysical properties of the lithosphere, particularly during serpentinization of peridotite. Mantle seismic velocities have been determined at depths as shallow as several hundred meters below seafloor beneath the central dome of Atlantis Massif. Drilling therefore offers an unprecedented opportunity to document relationships between the degree and chemistry of alteration and changes in geophysical properties and to describe the petrologic sequence that occurs across the Mohorovicic discontinuity (Moho) at this location. The potential for recovering unaltered peridotite at Atlantis Massif presents excellent opportunities for advances in understanding residual modes and microstructures associated with mantle flow and melt extraction within the oceanic mantle.

SCHEDULE FOR EXPEDITIONS 304 AND 305

Expeditions 304 and 305 are based on Integrated Ocean Drilling Program (IODP) drilling proposal number 512-Full3 (available at **www.isas-office.jp/scheduled.html**). Following ranking by the IODP Scientific Advisory Structure, the expeditions were scheduled by the IODP Operations Committee for the research vessel *JOIDES Resolution*, operating under contract with the U.S. Implementing Organization (USIO). Expedition 304 is currently scheduled to depart Ponta Delgado, Azores Islands (Portugal), on 14 November 2004 and to end in Ponta Delgado on 5 January 2005. A total of 52 days will be available for the drilling, coring, and downhole measurements described in this report. Expedition 305 is currently scheduled to depart Ponta Delgado, Azores Islands (Portugal), on 5 January 2005 and to end in Ponta Delgado on 27 February 2005. A total of 53 days will be available for the drilling, coring, and downhole measurements described in this report (for the current detailed schedule, see **iodp.tamu.edu/scienceops/**). Further details on the *JOIDES Resolution* can be found at **iodp.tamu.edu/publicinfo/drillship.html.**

GEOLOGIC SETTING

Results of Sea-Surface Mapping, Seismic, and Submersible Studies

The Atlantis Massif formed within the past 1.5–2 m.y., and it currently bounds the median valley of the Mid-Atlantic Ridge (MAR) on the west side. The corrugated, striated central portion of this domal massif displays morphologic and geophysical characteristics inferred to be representative of an oceanic core complex (OCC) exposed via long-lived detachment faulting (Fig. **F1**) (Cann et al., 1997; Blackman et al., 1998, 2004; Collins et al., 2001). The adjacent basaltic block to the east is interpreted as the hanging wall to the detachment fault. A thin cover of lithified sediment and rubble on the dome of the massif impedes seafloor mapping and sampling of the fault surface. Evolution of the southern portion of the massif differs somewhat from that of the central portion. The southern ridge (Fig. **F1**) has experienced greater uplift, shoaling to ≤700 m below sea level. At the southern ridge the corrugated surface extends eastward to the top of the median valley wall. Exposures along the south face of the massif represent a cross section through the core complex. The serpentinization-driven Lost City hydrothermal vent field is located just below the summit of the southern ridge (Kelley et al., 2001, 2003; Früh-Green et al., 2003).

The results of seismic refraction experiments at Atlantis Massif (Fig. **F2**) (Detrick and Collins, 1998) indicate that velocities of 8 km/s occur within several hundred meters of the seafloor in at least parts of the core of the massif. The gradient of seismic velocity in the central dome of Atlantis Massif is similar to that determined near Ocean Drilling Program (ODP) Site 920, where 100–200 m of serpentinized peridotite was drilled. The gradient is quite distinct from that characterizing gabbro-hosted Atlantis Bank (Southwest Indian Ridge) and other sections of the MAR.

Multichannel seismic reflection data (Fig. **F3**) show a major difference in structure of the outside (conjugate) corner lithosphere versus that hosting Atlantis Massif (Canales et al., 2004). The seismic Layer 2a/2b boundary is quite clear on the eastern flank of the ridge axis but it is not evident on the western flank where the massif occurs. A strong reflector is visible at 0.2–0.5 s below much of the domal surface (Fig. **F4**) and coincides with the depth below which mantle velocities (~8 km/s) are deduced. One interpretation suggests that the reflector marks an alteration front within the peridotite-dominated massif.

Modeling of sea-surface and sparse seafloor gravity data (Fig. **F5**) (Blackman et al., 1998, 2004; Nooner et al., 2003) suggests that there is a wedge-shaped body in the domal core with density 200–400 kg/m^3 greater than the surrounding rock. In the model, the footwall is overlain by tilted hanging wall blocks that are capped by material with density typical of upper crustal rock (2.5–2.7 kg/m^3). The interface between the model blocks on the east is a gently inclined (15°–25°) boundary that dips more steeply than the exposed corrugated surface (~11°) where it meets that hanging wall. It is likely that the density interface coincides with the base of the detachment fault zone, a region inferred to be highly altered and therefore of lower density. Sea-surface gravity data indicate that the extent of alteration within the southern ridge is greater than that of the central dome (Blackman et al., 2004).

In situ rock samples, side-scan imagery, and gravity data suggest that the majority of the hanging wall block comprises erupted basalt. Seismic data show a discontinuous but persistent reflector at 0.2–0.5 s beneath the seafloor (Fig. **F6**), which, according to Canales et al. (2004), coincides with the projection of the corrugated slope beneath the western edge of the hanging wall block. They interpret this reflector to be the unexposed detachment fault. Assuming an average velocity of 4 km/s in fractured basalt, the detachment is predicted to occur at 200–300 m depth below seafloor at the hanging wall drill site.

Rock samples collected by the manned submersible *Alvin* from the central dome are mostly angular talus and rubble of peridotite, metabasalt, and limestone (Cann et al., 2001; Blackman et al., 2004). A few samples showing cataclastic deformation fabrics or highly serpentinized and metasomatically altered peridotite were also recovered. The protolith of most of the serpentinite sampled on the south wall of the massif is harzburgite. These rocks are commonly cut by highly altered gabbroic veins composed dominantly of talc, tremolite, and chlorite (Früh-Green et al., 2001; Schroeder et al., 2001). Low-temperature overprinting, seafloor weathering, and carbonate vein formation mark the youngest phases of alteration.

Microstructural analysis of samples from the south wall indicates shear deformation and dilational fracturing at metamorphic conditions ranging from granulite to subgreenschist facies (Schroeder et al., 2001). Ductile fabrics in peridotite samples are overprinted by semibrittle and brittle deformation (Schroeder, 2003). Stable mineral assemblages of tremolite, chlorite, and chrysotile indicate that the latter process occurred at <400°C. The distribution of samples suggests that strong semibrittle and brittle deformation is concentrated at shallow structural levels (<90 m beneath the domal surface) at the southern ridge (Schroeder, 2003). Outcrop mapping with the *Alvin* and photomosaics constructed from Argo digital still camera images show that this uppermost fault extends across much of the top of the southern ridge (Karson, 2003).

SCIENTIFIC RATIONALE FOR DRILLING

Atlantis Massif has several key features that make it an ideal target for OCC drilling. The massif is <2 Ma, so weathering and erosion have not degraded (macro)structural relationships. The hanging wall is in contact with the footwall (core) of the detachment fault. The core of the massif is dominated by variably serpentinized peridotite at the surface, and mantle seismic velocity has been reported to occur at several hundred meters depth below seafloor, affording access to fresh in situ mantle with conventional drilling; therefore, we can document the alteration gradient and front with depth. Our scientific objectives cannot be accomplished via seafloor mapping/sampling.

Hypotheses

The hypotheses that drilling results will test are listed below, followed by the specific observations/measurements expected to be most critical. Whereas many of the obser-

vations and measurements outlined below will be initiated at sea, most of the results will be ascertained only after postcruise research programs.

1. *A major detachment fault system controlled the tectonic and metamorphic evolution of Atlantis Massif:*

   - thickness of the fault zone
   - ductile-brittle evolution
   - temperature and pressure conditions of equilibrium mineral assemblages
   - relationships between deformation and recrystallization
   - history of strain localization within the fault zone

   If core is recovered from within the detachment fault zone we will use micro- and macrostructural measurements to estimate the sense and magnitude of slip that has occurred on single slip surfaces and detail the occurrences of multiple slip planes that may work together to accommodate extension/plate spreading. The volume, structure, and composition of alteration products within the fault zone will provide constraints on slip accommodation and fluid flow along the fault. Observations of the lower boundary of the tectonized zone will be important for understanding whether strain is isolated or more distributed throughout the rocks some distance below the detachment (e.g., Fletcher and Bartley, 1994). Logging data will play a key role in understanding the detachment fault zone because recovery is likely to be poor due to the highly fractured nature of the rock. Downhole changes in fracture patterns, porosity, resistivity, and magnetic susceptibility will aid discrimination of fault zone structure and its variation with depth.

   The history of exposure of the detachment fault at the seafloor may be reflected by paleoceanographic indicators within sediments that drape the footwall. Sedimentation rates at 30°N in the Atlantic Ocean are sufficiently high that basement rock exposure on the dome is quite rare. Recovery of the thin (~1 m) lithified sediment section may provide constraints on the timing of footwall exhumation, which occurred over an unknown period in the past 1–2 m.y. In a given location, recovery of the topmost deposits would indicate microfossil and oceanographic (temperature and stable isotope) signatures characteristic of the deposition time. Recovery from a series of relatively shallow or bit-to-destruction spreading-parallel sites spanning the central dome could provide limits on the rate of unroofing (systematic changes in indicators from west to east) and perhaps on the time of initial fault exposure (age of the sediments on the western edge of the dome). Comparison of the top sediments at

the central dome to those on the southeast shoulder could address questions about differing evolution of these two portions of the detachment fault system (Blackman et al., 2004).

2. *Plate flexure (rolling hinge model) is the dominant mechanism of footwall uplift:*

- depth distribution of deformation degree/style
- localization of deformation
- alteration concentrated in local zones
- brittle deformation dominant in hanging wall
- rotation of tectonic blocks

If long-lived normal faulting and displacement are responsible for the evolution of the massif, uplift of the core may be the result of isostatic adjustment (Vening Meinesz, 1950) and thin-plate flexure (Spencer, 1985; Wernicke and Axen, 1988; Buck, 1988; Lavier et al., 1999). In this scenario, the pattern of footwall strain should vary from extension near the upper surface, through an interval of no evident strain, to compression in the lower part of the plate. Differential rotation between the footwall and hanging wall blocks is predicted by thin-plate theory, so we will investigate whether the core or logging data show evidence of such history. Logging data will provide continuous (orientated) images of fracture patterns in the borehole wall. These data will be compared with fractures and veins measured in the cores from the same depth interval. With constraints on core orientation and logging tool calibration, paleomagnetic data can be related (MacLeod et al., 1994, 1995) to any systematic rotation of the footwall and hanging wall.

3. *Significant unroofing occurs during formation of oceanic core complexes:*

- fluid inclusion analyses
- metamorphic history
- thermochronometry and thermal evolution

Gabbro is interlayered with peridotites along the south wall of the massif, and the core of the massif is likely composed of similar rock types. Fluid inclusions within gabbro can be used to determine the depth at which the rock formed (i.e., the pressure and temperature at which the fluid was entrapped) (e.g., Kelley and Delaney, 1987; Kelley and Früh-Green, 2001). Comparison of such data with the present depth of core samples can provide limits on the amount of uplift/unroofing. The pressure/tem-

perature evolution of metamorphism will reflect the tectonic evolution as well, with cooling rates and water/rock ratios being controlled by the amount of unroofing together with degree of fracturing. The detachment model predicts that the hanging wall basalts initially overlay the footwall. If this is the case, petrological and geochemical results are expected to show a genetic relationship between footwall peridotites, any melt residue therein, and the basalts of the hanging wall. Rock recovered via coring will allow this prediction to be tested.

4. *Expansion associated with serpentinization contributes significantly to uplift of core complexes:*

- distribution of alteration above serpentinization front
- orientation of deformation fabrics at angles to plate spreading direction
- evidence for significant rock-seawater exchange
- timing of alteration with respect to deformation
- microstructural analysis

If expansion of serpentinized peridotite contributed significantly to the evolution of the massif, the bulk density of the altered material must be low enough to allow it to move relative to the surrounding rock. Plastic flow structures within the serpentinite might reflect significant vertical shear, due to buoyancy of the expanding material.

5. *The Mohorovicic discontinuity (Moho) at Atlantis Massif is a hydration front:*

- link seismic velocity gradient to vertical distribution of rock types
- degree/distribution of alteration and cracking

Serpentinization of olivine in lower crustal and upper mantle rock types is associated with the uptake and release of both major and minor elements and compounds, including H_2O, Mg, Ca, Si, Cl, and B, which has important consequences for long-term global geochemical fluxes. Besides the production of heat through exothermic reactions, serpentinization leads to reduced, high-pH fluids with high H_2 and CH_4 concentrations. Recovery of this transition will allow quantitative modeling of geochemical changes associated with progressive serpentinization. As yet, the end-member compositions, and therefore geochemical fluxes associated with serpentinization, have been necessarily inferred from primary mineral modes and compositions.

6. *Nature of melting and/or magma supply contributes to episodes of long-term faulting:*

- variations in degree of melting, distribution of retained melt, and/or melt-rock reaction as functions of depth
- final depth of melting
- relationship between magmatism and subsolidus deformation

The processes responsible for the development of oceanic core complexes appear to be episodic, with one factor being the level or style of magmatic activity at the local spreading center. Evaluation of the degree of mantle melting the peridotites have undergone can be estimated from reconstructed residual mode and bulk rock (major element) chemistry and from major and trace element mineral chemistry (Cr# in spinel and pyroxenes, Mg# in olivine, TiO_2 in orthopyroxene and clinopyroxene, and heavy rare earth elements in clinopyroxene [Hellebrand et al., 2001]). Melts retained within residual peridotite may reflect in situ partial melting (Elthon, 1992) or transient melts ascended from deeper levels. This melt may react extensively with or otherwise refertilize the peridotite, altering both melt and residue compositions (e.g., Daines and Kohlstedt, 1994; Edwards and Malpas, 1996; Elthon, 1992; Johnson and Dick, 1992; Kelemen et al., 1992, 1997; Seyler and Bonatti, 1997; Seyler et al., 2001). Dissolution textures and mineral inclusions allow evaluation of the nature and amount of melt-rock interaction.

7. *Positive gravity anomalies at Atlantis Massif indicate relatively fresh peridotite:*

- core lithology and degree of alteration
- presence/lack of significant iron oxide gabbro
- correlation with seismic velocity

Late-stage magmas containing significant proportions of Fe and Ti can be emplaced in the crust at irregular intervals (Agar and Lloyd, 1997; Natland et al., 1991), thereby increasing the overall density of the intruded body. In this case, both high and average (crustal) density material might be mainly gabbroic, but they would have different bulk properties. To date, seafloor samples from Atlantis Massif do not indicate that high densities evident in the MAR 30°N residual gravity (Fig. **F3**) (Blackman et al., 2004) are due to the presence of significant Fe-Ti gabbro. Although the densities of such oxidized rocks can be high, the seismic velocity is not increased correspondingly (Itturino et al., 1991; Miller and Christensen, 1997), so Fe-Ti gabbro would not cause the high velocities observed. However, only through drilling will it

be possible to determine what rock types and their relative degree of alteration generate the observed geophysical signals.

Qualitative inferences derived from seafloor mapping and sampling at Atlantis Massif can become quantitative constraints on models when drill core and logging measurements/analyses are available. Key insights into uppermost mantle processes and the effect of alteration on rheology and geochemistry will be obtained through comparison of core samples from this site and those drilled at ODP Sites 670, 920, and 895 and sites of Leg 209. If recovery at the footwall site is sufficient, we will obtain information on depth variation in preferred alignment of minerals associated with flow in the mantle; together with the distributed, shallow samples obtained during Leg 209, analysis of any systematics of fabric with respect to tectonic setting can be addressed. Data from Expeditions 304 and 305 may also contribute to such studies directly if contingency operations obtain core from site(s) offset along strike from the priority footwall site.

Data from Expeditions 304 and 305 will also be used to address what controls fault geometry and slip behavior at different types of OCCs. Drilling results from Atlantis Bank (Hole 735B) (Dick et al., 2000) and seafloor mapping/sampling results from the 15°45′N MAR complex (MacLeod et al., 2002; Escartin et al., 2003) suggest that the depth dependence and relative timing of brittle versus ductile deformation may differ between OCCs. New information from Godzilla Megamullion (Ohara et al., 2001, 2003) is also expected to be directly relevant to this question. Drilling results from Atlantis Massif will provide key data for comparison.

RATIONALE FOR ADCB ENGINEERING COMPONENT

The advanced diamond core barrel (ADCB) is a development technology undertaken by ODP and IODP staff to overcome challenges routinely encountered in hard rock coring. The ADCB is a mining-style, narrow-kerf, diamond-impregnated bit that employs high rotation speed abrasion cutting as opposed to heavy impact (jack hammer) roller cone technology. Development of ADCB technology is crucial to improving our ability to core in young ocean crust and achieving many of the lithosphere objectives outlined in the IODP Long-Range Plan.

In our development configuration, the ADCB is significantly different than other IODP coring systems. The bottom-hole assembly (BHA) employs 6.75 inch drill collars (as opposed to the more robust 8.25 inch collars used in rotary coring). This BHA fea-

tures a continuous, smooth outer surface (conventional BHAs have expanded thickness at the tool joints). Whereas this slickwall BHA likely contributes to more efficient operation (material falling into the hole can lodge against the upsets at tool joints in a conventional BHA, potentially leading to a pipe stuck in the hole), it is significantly weaker than a conventional BHA and cannot be used to initiate a hole. The inherent weakness of the tool joints requires that the ADCB be deployed in a predrilled hole deep enough to support the BHA. The bottom of the hole must be free of debris to ensure a flush contact of the bit with the formation.

The ADCB cuts a core with 44% greater volume than conventional coring, so our standard protocol is to cut 4.5 m long cores (to reduce the weight of the recovered core and facilitate core handling). This requires twice as many wireline runs as conventional rotary coring, thus potentially increasing overall operations time. In addition, maximizing recovery with the ADCB requires retrieving the core barrel when there are indications that the throat of the bit is clogged (restricted circulating seawater flow rates), potentially necessitating many more wireline trips and subsequent reduction of overall penetration rates.

The ADCB was deployed during two recent ODP expeditions, Legs 193 and 194. Although both of these applications were operations of opportunity and yielded design and deployment improvements, neither directly addressed tool development specifications. During Leg 193, the material cored with the ADCB was fractured, hydrothermally altered dacite. Whereas the ADCB outperformed conventional rotary drilling in terms of quantity and quality of recovery, the scientific objectives of the mission obviated optimizing circulating fluid flow rates and rotation speeds in favor of rapid penetration. During Leg 194, operations were in shallow water (more complex operations in terms of weight-on-bit fluctuations) and the drilling target was carbonate. In this environment, ADCB recovery was significantly better than extended core barrel (XCB) coring and somewhat better than rotary core barrel (RCB) coring.

For the continued development of this system, several parameters require testing and monitoring. Operations during Leg 193 suggested that recovery and/or rate of penetration may be improved by optimizing circulating fluid flow rates and bit rotation speeds. Testing this requires recovery of several cores while adjusting and monitoring these parameters. In addition, we need to determine if the active heave compensation system limits weight-on-bit variations to within operational tolerances in open ocean deepwater environments. Bit designs need to be tested in basalt, gabbro, and peridotite, the lithologies of interest at mid-ocean-ridge and deep ocean crust exposures.

The ADCB development work will take priority for as long as 3 days during Expedition 304. If results exceed those typically obtained with the RCB, additional use of the ADCB may be requested.

DRILLING STRATEGY

IODP Expeditions 304 and 305 were planned based on a single proposal to core in two fundamentally different hard rock environments. One site is in the hanging wall to a low-angle detachment fault that has exposed deep crustal rocks on the Mid-Atlantic Ridge flank. The second target is the footwall to this fault, where the deep ocean crust and upper mantle have been exhumed. Lithologies (beneath a 1–2 m thick carapace of carbonates) are expected to be fractured pillow basalt in the hanging wall and altered gabbro and variably serpentinized peridotite in the footwall. High recovery is a priority, so we have prepared all operations estimates with the intent to recover cores in nominally 4.5 m intervals (half cores). Both sites will have penetrations in excess of 200 m (>400 and >700 m, respectively), thus requiring the ability make multiple reentries into each borehole.

Installing reentry templates in hard rock has historically met with limited success, but toward the end of ODP some progress was made in the deployment of hammer-in casing and reentry funnel assemblies. Although these tools are still developmental and have not been deployed in basalt, gabbro, or peridotite, the operations team for Expeditions 304 and 305 considers a hard rock reentry system (HRRS) as the most viable approach to assuring installation of a reentry template. An alternative approach, if the HRRS is unsuccessful, would be to drill a large-diameter borehole, attempt a single bare hole reentry, and deploy a free-fall funnel with a short casing. Another constraint on our operations planning is the assumption that we are not likely to be able to reach our depth target in the footwall site (>700 m) in 40–41 operational days (scheduled time on site). It is possible to reach this target, however, if some time during Expedition 304 is allocated to hole preparation and uppermost section recovery for Expedition 305.

Drill Sites

Primary Site: Proposed Site AMFW-01A

Our first occupation during Expedition 304 will be the footwall site (proposed Site AMFW-01A) (Table **T1**). We will attempt a pilot hole, coring to ~130 meters below sea-

floor (mbsf) to ensure we have selected a drilling location consistent with our objectives (the sediment cover precludes direct observation and we would prefer to avoid initiating a hole with casing in basaltic rubble). Conventional rotary coring (with the exception of recovering 4.5 m cores) to this depth will provide information on formation integrity for our casing deployment and will be sufficient for a wireline logging program in the upper part of the corrugated dome. The goal of ~130 mbsf is also the maximum depth we are likely to reach on a single bit run. Once we have established a deep-penetration drilling target, we will offset a few meters and deploy the HRRS with large-diameter casing to nominally 20 mbsf. A large-diameter hole will then be drilled to ~130 mbsf, and casing will be installed to within a few meters of the bottom of the hole (~120 mbsf) to ensure the upper part of the borehole will not collapse. This will complete our optimum operations strategy at the footwall site during Expedition 304.

Primary Site: Proposed Site AMHW-01A

Once we have established the reentry template in the footwall site, we will make the short transit to the hanging wall site (proposed Site AMHW-01A) and complete operations there. At proposed Site AMHW-01A, the HRRS will be set to ~20 mbsf (since we have no reason to believe anything but basalt is present in the hanging wall, no pilot hole is required). Conventional rotary coring (with the exception of recovering cores in 4.5 m increments) will follow to a depth of ±70 mbsf. The ADCB will be used to deepen the hole to ±130 mbsf. Since it is likely the borehole walls will be unstable in fractured basalt, we expect to open the borehole and install a casing string to ~120 mbsf. With the remaining time during Expedition 304, the borehole at proposed Site AMHW-01A will be deepened, targeting penetration through the detachment fault. Operations during Expedition 304 will conclude with multiple logging runs at this site.

Return to Proposed Site AMFW-01A

The operational strategy for Expedition 305 is straightforward (Table **T2**). After reoccupying the borehole in the footwall (proposed Site AMFW-01A), we will core as deep as possible, leaving sufficient time at the end of coring to allow for multiple logging runs, including a borehole vertical seismic profile experiment. It is possible that an array of ocean bottom seismometers (OBS) may be deployed near our drill site as part of a seismic-while-drilling experiment. A few hours of operations time may be sequestered at the conclusion of coring and downhole experiments to recover these OBS.

Contingency Strategies

Owing to the inherent risks of hard rock coring, we have developed plans for alternative operations. Achieving the target at proposed Site AMFW-01A is a high priority for the project. Since it is relatively deep and reaching that target relies on at least some preparation during Expedition 304, we have elected to begin operations during Expedition 304 at this site. Our contingency strategy allows for multiple time-dependent options based on the level of operational success achieved.

If the pilot hole at the footwall site fails to reach a depth sufficient to reach the objectives outlined in our primary operations plan, it should be early enough in the expedition to attempt another pilot hole within the same operational area (proposed Site AMFW-01A). Our strategy will be to continue attempts to establish a pilot hole until successful or until 12 days on site have expired (leaving the required 28 days to complete operations at the proposed hanging wall Site AMHW-01A). Once the pilot hole is successful (including multiple logging tool runs if possible), we will complete as much of the casing operation at an adjacent HRRS site as possible until time constraints require us to move to the hanging wall site.

Since establishing a reentry template during Expedition 304 is important to the objectives of Expedition 305, in the event of failure of the first HRRS site (according to our primary operations plan this could occur during coring or casing attempts), we expect to attempt to set a second HRRS nearby, if the cause of failure of the initial deep penetration borehole does not preclude a second attempt. We will conclude as much of this operation as possible before moving to the hanging wall site in time to achieve complete operations there.

If attempts to reach the detachment fault at the hanging wall are unsuccessful, we will not attempt to deploy a second reentry template; doing so would not leave enough time for the target depth to be reached at that site. The objective of penetrating the unexposed detachment fault during Expedition 304 is likely to be abandoned if the original drilling strategy at proposed Site AMHW-01A fails.

Two options that we consider important to completing the other objectives of these expeditions are to return to the footwall and either continue deepening the existing borehole (or completing casing operations if required) or to attempt to recover the uppermost carapace of the footwall (see **"Scientific Rationale for Drilling"**). This can be accomplished via a few short offset holes or a transect of spreading direction–parallel shallow-penetration holes within a few kilometers of the primary footwall

site, possibly recovered with XCB or motor-driven core barrel technology. A decision on which of these options to pursue will depend on the time remaining in the expedition.

Contingency planning for Expedition 305 also presents a series of options if the deep-penetration hole fails; the choice would be based on the amount of time remaining. Our first-priority alternative is to attempt another deep-penetration site. However, a minimum of 35 days is required to reach 800 mbsf and 27 days is required to reach 600 mbsf. If the failure occurs more than a week into Expedition 305, we will not likely be able to attain 800 mbsf. If there is insufficient time to reach our depth target, several of the primary objectives of the expeditions can be addressed by a series of single-bit or shallow-penetration holes. If time is available, we will consider a transect of penetration-to-bit-destruction holes on the central dome of the footwall, including logging operations if possible. Our highest-priority transect would be a spreading direction–parallel series of holes (see **"Scientific Rationale for Drilling"**). If time is still available, we would also consider a transect of strike-parallel holes. If only a short time is available, we would consider a series of short offset holes to recover the upper carapace of the central dome or, potentially, the southeast shoulder of the massif.

The number of contingency sites and the order in which they might be occupied will depend on objectives achieved or addressed at the primary sites. We intend to occupy the alternate sites only if there is insufficient time or tools to complete our deep-penetration targets. As stated above, our highest priority alternate target is a spreading direction–parallel transect across the dome. One, two, or three locations (proposed Sites Alt AMFW-02A, 03A, and 04A) might be drilled along seismic Line Meg-10 (Figs. **F4, F7**). As each occupation will take 3–5 days (cored to bit destruction; see Table **T2**), the number of sites (and thus the specific locations) cannot be defined with certainty until the amount of time available is determined. With only a few days (<5) available, the most likely scenario, given our current information, would be to select a target near the western end of our transect. Ultimately, the targets selected for drilling will be determined by discussion among the science coordination team at sea (Co-chief Scientists, Staff Scientist, and Operations Superintendent), the operations team on shore for the companion expedition, and IODP-TAMU management with communication through IODP-TAMU Headquarters to IODP Management International.

In the event there is sufficient time to complete the objectives of the spreading parallel–direction transect, the next priority contingency operation is targets (one or two

depending on time available) along the massif parallel to the ridge axis. Structure at these alternate sites is illustrated in Figure **F8** (proposed Sites Alt AMFW-05A and 06A) along seismic Line Meg-4. The specific location of these targets will depend on the results of previous operations and a subsea camera survey.

The final contingency site we include (proposed Site Alt AMFW-07A) is the potential of shallow penetration (a few meters) on the southeast shoulder of the Atlantis Massif, located along seismic Line Meg-9 (Figs. **F7, F8**), for comparison to the surface of the detachment fault at other sites on the northern limb of the massif.

In the event of catastrophic failure of either deep-penetration site, we can still achieve some of the science objectives of these expeditions if the resistivity-at-the-bit (RAB) logging-while-drilling tool is available. If this tool can only be available for a single expedition, we prefer to have it on Expedition 305 as an ultimate option if all attempts to core and log through the detachment or into the central dome have been unsuccessful (see **"Logging Strategy"**).

SAMPLING PLAN

Shipboard and shore-based researchers should refer to the interim IODP Sample, Data, and Obligations policy posted on the Web at **iodp.tamu.edu/curation/policy.html.** This document outlines the policy for distributing IODP samples and data to research scientists, curators, and educators. The document also defines the obligations that sample and data recipients incur. Owing to the unprecedented scheduling of two consecutive expeditions from a single proposal, the Science Planning Committee of IODP has recommended that the science parties of both expeditions be considered a single entity. Therefore, the Sample Allocation Committee (SAC) will consist of all four Co-Chief Scientists, both Staff Scientists, the IODP onshore Curator, and the curatorial representatives onboard ship. This team will work with the entire science party from both expeditions to formulate a specific sampling plan for shipboard and postcruise sampling.

In order to coordinate all shipboard sampling, shipboard scientists from both expeditions are expected to submit sample requests (**iodp.tamu.edu/curation/samples.html**) no later than 2 months before the beginning of the first expedition. Based on sample requests (shipboard and shore based) submitted by this deadline, the SAC will prepare a tentative sampling plan. The sampling plan will be subject to modifi-

cation depending upon the actual material recovered and collaborations that may evolve between scientists during the expeditions.

Based on prior results coring serpentinized peridotite during ODP Legs 153 and 209, we expect to recover 500–700 m of core during the two expeditions (as much as 400 m of serpentinized peridotite and lesser gabbro and, possibly, 200 m of basalt). The minimum permanent archive will be the standard archive half of each core. Samples for shipboard studies will be collected routinely (likely daily) following core labeling, nondestructive whole-core measurements (multisensor track measurements and possibly whole-core images), core splitting, close-up photography of intervals of interest, and core description. Shipboard samples for geochemical, mineralogical, and fabric analyses and for physical property measurements will be extracted from working halves of cores by the shipboard party. When possible, our goal will be to make as many measurements as possible on common samples, thus reducing the amount of material removed from the core and enhancing the opportunity for data correlation.

In order to provide the entire science party access to the cores from both expeditions and the opportunity to formulate sampling strategies based on the entire recovery, sampling for postcruise research must take place on shore after the second expedition. Some personal sampling for ephemeral properties, microbiology, and/or whole-round samples will take place during each expedition; however, the bulk of personal sampling will take place at a shore-based repository. Although the cores from these expeditions will eventually be stored at the Bremen Core Repository (Germany), for logistical reasons the cores will be shipped directly to the Gulf Coast Repository at Texas A&M University (TAMU; USA), which is better equipped to handle a postcruise sampling program of this magnitude. The most convenient and cost-effective time to hold this sampling party would be in conjunction with the postcruise meeting held at IODP-TAMU for editing the expedition report, ~3 months after the end of Expedition 305. Coordination between the science parties will be accomplished by the SAC, and preparation of detailed records for preferred sampling intervals of each participant will be done during the expeditions. With this preparation, a 3–4 day meeting at the Gulf Coast Repository, with all sampling participants from both expeditions including approved shore-based researchers, should be sufficient for completion of all tasks. This time estimate is based on the single sampling party held at the conclusion of ODP Leg 209, where nearly 400 m of core was sampled.

For the purpose of developing sample requests, participating scientists could expect to receive on the order of 25–100 samples of no more than 15 cm^3. This is based on

historic precedent from ODP designed to enable scientists to complete a research program and meet the established publication deadlines. For these expeditions, all personal sample frequencies and sample volumes taken from the working half of the core must be justified on a scientific basis and will be dependent on core recovery, the full spectrum of other requests, and the project objectives. Postcruise research projects that require more frequent sampling or larger sample volumes should be further justified in sample requests. Some redundancy of measurement is unavoidable, but minimizing redundancy of measurements among the shipboard party and identified shore-based collaborators will be a factor in evaluating sample requests.

If some critical intervals are recovered (e.g., fault gouge, veins, fresh peridotite, gabbroic intervals, melt lenses, etc.), there may be considerable demand for samples from a limited amount of cored material. These intervals may require special handling, a higher sampling density, reduced sample size, or continuous core sampling by a single investigator. A sampling plan coordinated by the SAC may be required before critical intervals are sampled.

LOGGING STRATEGY

Our logging strategy is designed to complement and complete our overall cruise objectives, determining the lithology, orientation of deformation fabrics, and proportions and orientation of features. Downhole logging may provide our only continuous record because of the potential of low core recovery. A main objective of the wireline logging program will be to orient faults, fractures, and deformation features using borehole imaging techniques. Borehole images may then help orient core pieces or sections if the core recovery is sufficiently high. In addition to defining structural features, the logging program will also attempt to establish lithologic or physical property boundaries, as interpreted from logging tool response characteristics as a function of depth; determine serpentinization and/or alteration patterns in basalts, lower crustal, and upper mantle rocks; and produce direct correlations with discrete laboratory measurements on the recovered core.

Because of its potential impact on achieving cruise objectives, we have scheduled time for downhole logging operations at hanging wall and footwall sites (pilot and cased holes). Five tool strings will be deployed: triple combination (triple combo) tool string, Formation MicroScanner/Dipole Sonic Imager (FMS/sonic) tool string, Ultrasonic Borehole Imager (UBI), borehole magnetometer, and Well Seismic Tool

(WST). Additionally, our contingency plan calls for use of the RAB tool to drill to bit destruction at an alternate hanging wall (and possibly footwall) site.

Triple Combination Tool String

Data from the triple combo will provide continuous measurement of the natural radioactivity and Th, U, and K contents (Hostile Environment Gamma Ray Sonde), density (Hostile Environment Litho-Density Sonde), neutron porosity (Accelerator Porosity Sonde), electrical resistivity (Dual Laterolog), and temperature profiles (Temperature/Acceleration/Pressure tool). These measurements will be utilized for the characterization of changes in lithology (gabbros versus peridotites) and variations in alteration (fresh to serpentinized peridotites).

Formation MicroScanner/Dipole Sonic Imager Tool String

The FMS/sonic tool string has two main components:

- The FMS provides high-resolution electrical images of the penetrated formations. These images will be utilized for the characterization of lithologic sequences and boundaries, oriented fracture patterns, fracture apertures, and fracture densities. FMS images can be used to visually compare logs with core to ascertain the orientations of bedding and fracture patterns.
- The Dipole Shear Sonic Imager (DSI) will produce a full set of waveforms (*P*-, *S*-, and Stoneley waves). Cross-dipole shear wave velocities measured at different azimuths may be used to determine preferred mineral, fracture, and/or fabric orientations that may produce seismic velocity anisotropy.

Ultrasonic Borehole Imager

The UBI measures the amplitude and transit time of an acoustic wave propagated into the formation. It provides high-resolution images with 100% borehole wall coverage, which allows detection of small-scale fractures. The amplitude depends on the reflection coefficient of the borehole fluid/rock interface, the position of the UBI tool in the borehole, the shape of the borehole, and the roughness of the borehole wall. Changes in the borehole wall roughness (e.g., at fractures intersecting the borehole) are responsible for the modulation of the reflected signal; therefore, fractures or lithologic variations can easily be recognized in the amplitude image. The General Purpose Inclinometer Tool (GPIT) is deployed with the UBI and allows orientation of the images; evaluation and orientation of fractures can provide information about the

local stress field and borehole geometry. Deployment of the UBI is contingent on availability of funds.

Borehole Magnetometer

The Göttingen Borehole Magnetometer (GBM) previously deployed during ODP Leg 197 will be available as a third-party tool during Expedition 305. This tool has three fluxgate sensors that measure three orthogonal components of the magnetic field. The tool includes a gyroscope, which measures the tool rotation during data acquisition and allows the orientation of the tool to be determined. The data from the magnetometer will be used to monitor changes in the magnetic properties of the oceanic lithosphere as well as changes in paleomagnetic direction that can aid in determination of the magnetic polarity.

Three-Component Well Seismic Tool

The WST-3 records acoustic waves generated by an air gun or water gun located near the sea surface. It provides a complete checkshot survey and a depth-traveltime plot; synthetic seismograms will be essential for determining in situ velocity profiles.

Resistivity-at-the-Bit Tool

The RAB has been requested as part of our contingency strategy for Expedition 305. The strategy for using the RAB will be determined on the basis of the ability to obtain wireline logs at the hanging wall site. Deployment of the RAB is contingent on availability of funds.

The RAB will provide borehole resistivity logs and images at three different depths of investigation and total gamma ray logs. The RAB measures oriented resistivity images of the borehole wall, similar to an FMS wireline tool. These fracture orientations and distributions can be observed as resistivity contrasts in the image logs and are critical for recognizing the extent of the deformation structures. These data will provide visual recognition of igneous layers as well as the identification of fracture patterns, structural orientations, and formation thicknesses. These oriented images could be critical for a assessing the structure within the uppermost 80 m of the borehole since the RAB is the only tool able to record such oriented images.

REFERENCES

Agar, S.M., and Lloyd, G.E., 1997. Deformation of Fe-Ti oxides in gabbroic shear zones from the MARK area. *In* Karson, J.A., Cannat, M., Miller, D.J., and Elthon, D. (Eds.), *Proc. ODP, Sci. Results*, 153: College Station, TX (Ocean Drilling Program), 123–141.

Blackman, D.K., Cann, J.R., Janssen, B., and Smith, D.K., 1998. Origin of extensional core complexes: evidence from the MAR at Atlantis Fracture Zone. *J. Geophys. Res.*, 103:21315–21334.

Blackman, D.K., Karson, J.A., Kelley, D.S., Cann, J.R., Früh-Green, G.L., Gee, J.S., Hurst, S.D., John, B.E., Morgan, J., Nooner, S.L., Ross, D.K., Schroeder, T.J., and Williams, E.A., 2004. Geology of the Atlantis Massif (MAR 30°N): implications for the evolution of an ultramafic oceanic core complex. *Mar. Geophys. Res.*, 23:443–469.

Buck, W.R., 1988. Flexural rotation of normal faults. *Tectonics*, 7:959–973.

Canales, J.-P., Tucholke, B.E., and Collins, J.A., 2004. Seismic reflection imaging of an oceanic detachment fault: Atlantis megamullion (Mid-Atlantic Ridge, 30°10′N). *Earth Planet. Sci. Lett.*, 222:543–560.

Cann, J., Blackman, D., Morgan, J., and *MARVEL* cruise participants, 2001. Geological inferences about the Mid-Atlantic Ridge 30°N core complex from initial analysis of side-scan, bathymetry and basalt petrography. *Eos, Trans. Am. Geophys. Union*, 82:F1099.

Cann, J.R., Blackman, D.K., Smith, D.K., McAllister, E., Janssen, B., Mello, S., Avgerinos, E., Pascoe, A.R., and Escartin, J., 1997. Corrugated slip surfaces formed at ridge-transform intersections on the Mid-Atlantic Ridge. *Nature*, 385:329–332.

Collins, J.A., Tucholke, B.E., and Canales, J.-P., 2001. Structure of Mid-Atlantic Ridge megamullions from seismic refraction experiments and multichannel seismic reflection profiling, *Eos, Trans. Am. Geophys. Union*, 82:F1100.

Daines, M.J., and Kohlstedt, D.L., 1994. The transition from porous to channelized flow due to melt/rock reaction during melt migration. *Geophys. Res. Lett.*, 21:145–148.

Detrick, R.S., and Collins, J.A., 1998. Seismic structure of ultramafics exposed at shallow crustal levels in the Mid-Atlantic Ridge rift valley at 15°N. *Eos, Trans. Am. Geophys. Union*, 79:F800.

Dick, H.J.B., Natland, J.H., Alt, J.C., Bach, W., Bideau, D., Gee, J.S., Haggas, S., Hertogen, J.G.H., Hirth, G., Holm, P.M., Ildefonse, B., Iturrino, G.J., John, B.E., Kelley, D.S., Kikawa, E., Kingdon, A., LeRoux, P.J., Maeda, J., Meyer, P.S., Miller, D.J., Naslund, H.R., Niu, Y.-L., Robinson, P.T., Snow, J., Stephen, R.A., Trimby, P.W., Worm, H.-U., and Yoshinobu, A., 2000. A long in situ section of the lower ocean crust: results of ODP Leg 176 drilling at the Southwest Indian Ridge. *Earth Planet. Sci. Lett.*, 179:31–51.

Edwards, S.J., and Malpas, J., 1996. Melt-peridotite interactions in shallow mantle at the East Pacific Rise: evidence from ODP Site 895 (Hess Deep). *Mineral. Mag.*, 60:191–206.

Elthon, D., 1992. Chemical trends in abyssal peridotites: refertilization of depleted suboceanic mantle. *J. Geophys. Res.*, 97:9015–9025.

Escartin, J., Mével, C., MacLeod, C.J., and McCaig, A., 2003. Constraints on deformation conditions and the origin of oceanic detachments, the Mid-Atlantic Ridge core complex at 15°45′N. *Geochem., Geophys., Geosyst.*, 4:10.1029/2002GC000472.

Fletcher, J.M., and Bartley, J.M., 1994. Constrictional strain in a non-coaxial shear zone: implications for fold and rock fabric development, central Mojave metamorphic core complex, California. *J. Sruct. Geol.*, 16:555–570.

Früh-Green, G., Kelley, D.S., Karson, J.A., Blackman, D.K., Boschi, C., John, B.E., Schroeder, T., Ross, D.K., and *MARVEL* cruise participants, 2001. Hydrothermal alteration, serpentinization and carbonate precipitation at the Lost City vent field (30°N MAR). *Eos, Trans. Am. Geophys. Union*, 82:F1101.

Früh-Green, G.L., Kelley, D.S., Bernasconie, S.M., Karson, J.A., Ludwig, K.A., Butterfield, D.A., Boschi, C., and Proskurowksi, G., 2003. 30,000 years of hydrothermal activity at the Lost City vent field. *Science*, 301:495–498.

Hellebrand, E., Snow, J.E., Dick, H.J.B., and Hofmann, A.W., 2001. Coupled major and trace elements as indicators of the extent of melting in mid-ocean-ridge peridotites. *Nature*, 410:677–681.

Iturrino, G.J., Christensen, N.I., Kirby, S., and Salisbury, M.H., 1991. Seismic velocities and elastic properties of oceanic gabbroic rocks from Hole 735B. *In* Von Herzen, R.P., Robinson, P.T., et al., *Proc. ODP, Sci. Results*, 118: College Station, TX (Ocean Drilling Program), 227–244.

Johnson, K.T.M., and Dick, H.J.B., 1992. Open system melting and temporal and spatial variation of peridotite and basalt at the Atlantis II Fracture Zone. *J. Geophys. Res.*, 97:9219–9241.

Karson, J.A., 2003. Unconformities in slow-spread oceanic crust: implications for spreading processes and dismembered ophiolites. *Eos, Trans. Am. Geophys. Union*, 84:F1506.

Kelemen, P.B., Hirth, G., Shimizu, N., Spiegelman, M., and Dick, H.J.B., 1997. A review of melt migration processes in the asthenospheric mantle beneath oceanic spreading centers. *Philos. Trans. R. Soc. London, Ser. A*, 355:283–318.

Kelemen, P.B., Quick, J.E., and Dick, H.J.B., 1992. Formation of harzburgite by pervasive melt/rock reaction in the upper mantle. *Nature*, 358:635–641.

Kelley, D.S., and Delaney, J.R., 1987. Two-phase separation and fracturing in mid-ocean ridge gabbros at temperatures greater than 700°C. *Earth Planet. Sci. Lett.*, 83:53–66.

Kelley, D.S., and Früh-Green, G., 2001. Volatile lines of descent in submarine plutonic environments: insights from stable isotope and fluid inclusion analyses. *Geochim. Cosmochim. Acta*, 65:3325–3346.

Kelley, D.S., Karson, J.A., Blackman, D.K., Früh-Green, G.L., Butterfield, D.A., Lilley, M.D., Olson, E.J., Schrenk, M.O., Roe, K.K., Lebon, G.T., Rivizzigno, P., and Shipboard Party, 2001. An off-axis hydrothermal vent field near the Mid-Atlantic Ridge at 30°N. *Nature*, 412:123–128.

Kelley, D.S., Karson, J.A., Yoerger, D., Früh-Green, G.L., Butterfield, D.A., and Lilley, M., 2003. Discovering new mantle-hosted submarine ecosystems: the Lost City hydrothermal field. *Eos, Trans. Am. Geophys. Union*, 84:F230.

Lavier, L., Buck, W.R., and Poliakov, A.N.B., 1999. Self-consistent rolling-hinge model for the evolution of large-offset low-angle normal faults. *Geology*, 27:1127–1130.

MacLeod, C.J., Célérier, B., and Harvey, P.K., 1995. Further techniques for core reorientation by core-log integration: application to structural studies of the lower oceanic crust in Hess Deep, eastern Pacific. *Sci. Drill.*, 5:77–86.

MacLeod, C.J., Escartin, J., Banerji, D., Banks, G.J., Gleeson, M., Irving, D.H.B., Lilly, R.M., McCaig, A.M., Niu, Y., Allerton, S., and Smith, D.K., 2002. Direct geological evidence for oceanic detachment faulting: the Mid-Atlantic Ridge, 15°45′N. *Geology*, 30:879–882.

MacLeod, C.J., Parson, L.M., and Sager, W.W., 1994. Reorientation of core using the Formation MicroScanner and Borehole Televiewer: application to structural and palaeomagnetic studies with the Ocean Drilling Program. *In* Hawkins, J., Parson, L., Allan, J., et al., *Proc. ODP, Scientific Results*, 135: College Station, TX (Ocean Drilling Program), 301–311.

Miller, D.J., and Christensen, N.I., 1997. Seismic velocities of lower crustal and upper mantle rocks from the slow-spreading Mid-Atlantic Ridge, south of the Kane Transform Zone (MARK). *In* Karson, J.A., Cannat, M., Miller, D.J., and Elthon, D. (Eds.), *Proc. ODP, Sci. Results*, 153: College Station, TX (Ocean Drilling Program), 437–454.

Natland, J.H., Meyer, P.S., Dick, H.J.B., and Bloomer, S.H., 1991. Magmatic oxides and sulfides in gabbroic rocks from Hole 735B and the later development of the liquid line of descent. *In* Von Herzen, R.P., Robinson, P.T., et al., *Proc. ODP, Sci. Results*, 118: College Station, TX (Ocean Drilling Program), 75–111.

Nooner, S.L., Sasagawa, G.S., Blackman, D.K., and Zumberge, M.A., 2003. Constraints on crustal structure at the Mid-Atlantic Ridge from seafloor gravity measurements made at the Atlantis Massif. *Geophys. Res. Lett.*, 30:10.1029/2003GL017126.

Ohara, Y., Fujioka, K., Ishii, T., and Yurimoto, H., 2003. Peridotites and gabbros from the Parece Vela backarc basin: unique tectonic window in an extinct backarc spreading ridge. *Geochem., Geophys., Geosys.*, 4:10.1029/2002GC000469.

Ohara, Y., Yoshida, T., Kato, Y., and Kasuga, S., 2001. Giant megamullion in the Parece Vela backarc basin. *Mar. Geophys. Res.*, 22:47–61.

Schroeder, T., John, B.E., Kelley, D., and *MARVEL* cruise participants, 2001. Microstructural observations of an "oceanic core complex": Atlantis Massif, 30°N Mid-Atlantic Ridge. *Eos, Trans. Am. Geophys. Union*, 82:F1100.

Schroeder, T.J., 2003. Modes and implications of mantle and lower-crust denudation at slow-spreading mid-ocean ridges. [Ph.D. dissert.], Univ. Wyoming, Laramie.

Seyler, M., and Bonatti, E., 1997. Regional-scale melt-rock interaction in lherzolitic mantle in the Romanche Fracture Zone (Atlantic Ocean). *Earth Planet. Sci. Lett.*, 146:273–287.

Seyler, M., Toplis, M.J., Lorand, J.-P., Luguet, A., and Cannat, M., 2001. Clinopyroxene microtextures reveal incompletely extracted melts in abyssal peridotites. *Geology*, 29:155–158.

Spencer, J.E., 1985. Miocene low-angle normal faulting and dike emplacement, Homer Mountain and surrounding areas, southeastern California and southernmost Nevada. *Geol. Soc. Am. Bull.*, 96:110–1155.

Vening Meinesz, F.A., 1950. Les graben africains resultant de compression oe de tension dans la croute terrestres? *Kol. Inst. Bull.*, 21:539–552.

Wernicke, B.P., and Axen, G.J., 1988. On the role of isostasy in the evolution of normal fault systems. *Geology*, 16:848–451.

Table T1. Operations summary and time estimates for Expedition 304.

Site	Location	Water depth (mbsl)	Operations description	Transit (days)	Drilling (days)	Logging (days)
Ponta Delgada, Azores			Sea voyage from Ponta Delgada to Site AMFW-01A, 936 nmi @ 10.5 kt	3.7		
AMFW-01A	30.170°N, 42.123°W	1630	Hole A: Bare rock spud, RCB 4.5 m cores 0–130 mbsf		3.1	
			Drop bit, log: triple combo, FMS/sonic, UBI			1.2
			Hole B: HRRS hammer drill-in 22 m of 13 3/8 inch casing		1.9	
			Underream 14 3/4 inch hole with bicenter bit to ~130 mbsf		3.1	
			Run 120 m of 10 3/4 inch casing with MM and underreamer		1.7	
			Set retainer, cement 10 3/4 inch casing **Subtotal = 11.9 days**		0.9	
			Transit from Site AMFW-01A to Site AMHW-01A, 3.3 nmi @ 1.0 kt	0.1		
AMHW-01A	30.192°N, 42.065°W	2580	Hole A: HRRS hammer drill-in 22 m of 13 3/8 inch casing		2.1	
			RCB 4.5 m cores 22–70 mbsf; ADCB 4.5 m cores 70–130 mbsf		4.4	
			Underream 14 3/4 inch hole with bicenter bit to ~130 mbsf		3.2	
			Run 120 m of 10 3/4 inch casing with MM and underreamer		1.8	
			Set retainer, cement 10 3/4 inch casing		0.9	
			Clean out cement, RCB 4.5 m cores 130–250 mbsf		4.7	
			RCB 4.5 m cores 250–370 mbsf		4.5	
			RCB 4.5 m cores 370–500 mbsf		4.2	
			Drop bit; log: triple combo, FMS/sonic, UBI **Subtotal = 27.6 days**			1.8
Ponta Delgada, Azores			Sea voyage from Site AMHW-01A to Ponta Delgada, 932 nmi @ 10.5 kt	3.7		
			Subtotal:	**7.5**	**36.5**	**3.0**
			Total days:		**47.0**	
Alternate operations						
If first footwall pilot hole fails (not peridotite/gabbro or bad hole conditions), attempt another pilot hole.						
Footwall peridotite	~30.17°N, ~42.12°W	~1630	Bare rock spud, RCB 4.5 m cores 0–130 mbsf		3.1	
			Drop bit; log: triple combo, FMS/sonic, UBI **Subtotal = 4.3 days**			1.2
If first footwall pilot hole OK but HRRS fails, attempt second HRRS installation and core (leave time for hanging wall site [27.6 days]).						
Footwall peridotite	~30.17°N, ~42.12°W	~1630	HRRS hammer drill-in 22 m of 13 3/8 inch casing		1.9	
			Underream 14 3/4 inch hole with bicenter bit to ~130 mbsf		3.1	
			Run 120 m of 10 3/4 inch casing with MM and underreamer		1.7	
			Set retainer, cement 10 3/4 inch casing **Subtotal = 7.6 days**		0.9	
If first footwall pilot hole and HRRS OK but first hanging wall HRRS fails (insufficient time to deploy second hanging wall HRRS), deepen footwall hole as time permits (no more than 18–20 days).						
Footwall peridotite	~30.17°N, ~42.12°W	~1630	Clean out cement, RCB 4.5 m cores 130–250 mbsf		4.2	
			RCB 4.5 m cores 250–370 mbsf **Subtotal = 8.3 days**		4.1	
			RCB 4.5 m cores 370–490 mbsf **Subtotal = 12.1 days**		3.8	
			RCB 4.5 m cores 490–610 mbsf **Subtotal = 16.4 days**		4.3	
			RCB 4.5 m cores 610–730 mbsf **Subtotal = 20.8 days**		4.4	
Transect of shallow MDCB core holes in footwall.						
Footwall peridotite	~30.17°N, ~42.12°W	~1630	Trip in/out with XCB/MDCB BHA		0.6	
			MDCB core two holes 0 to ~9.0 mbsf average **Subtotal = 1.3 days**		0.7	
Bare rock spud and RCB 4.5 m cores to bit destruction in footwall.						
Footwall peridotite	~30.17°N, ~42.12°W	~1630	RCB 4.5 m cores to bit destruction 0 to ~150 mbsf		3.9	
			Drop bit; log: triple combo, FMS/sonic, UBI **Subtotal = 5.5 days**			1.6
Shallow cores to recover upper part of footwall (detachment surface).						
Footwall peridotite	~30.17°N, ~42.12°W	~1630	RCB 4.5 m cores 0 to ~26 mbsf		1.6	
			Subtotal = 1.6 days			

Note: RCB = rotary core barrel, FMS = Formation MicroScanner, UBI = ultrasonic borehole imager, HRRS = hard rock reentry system, MM = mud motor, ADCB = advanced diamond core barrel, XCB = extended core barrel, MDCB = motor-driven core barrel, BHA = bottom-hole assembly.

Table T2. Operations summary and time estimates for Expedition 305.

Site	Location	Water depth (mbsl)	Operations description	Transit (days)	Drilling (days)	Logging (days)
Ponta Delgada, Azores			Sea voyage from Ponta Delgada to Site AMFW-01A, 936 nmi @ 10.5 kt	3.7		
AMFW-01A	30.170°N, 42.123°W	1630	Hole A: Bare rock spud, RCB 4.5 m cores 0–130 mbsf (3.1 days)			
			Drop bit, log: triple combo, FMS/sonic, UBI (1.2 days)			
			Hole B: HRRS hammer drill-in 22 m of 13 3/8 inch casing (1.9 days)			
			Underream 14 3/4 inch hole with bicenter bit to ~130 mbsf (3.1 days)			
			Run 120 m of 10 3/4 inch casing with MM and underreamer (1.7 days)			
			Set retainer, cement 10 3/4 inch casing (0.9 days)			
			Clean out cement, RCB 4.5 m cores 130–250 mbsf		4.2	
			RCB 4.5 m cores 250–370 mbsf		4.1	
			RCB 4.5 m cores 370–490 mbsf		3.8	
			RCB 4.5 m cores 490–610 mbsf		4.3	
			RCB 4.5 m cores 610–730 mbsf		4.4	
			RCB 4.5 m cores 730–850 mbsf		4.4	
			RCB 4.5 m cores 850–970 mbsf		4.5	
			RCB 4.5 m cores 970–1090 mbsf		4.7	
			RCB 4.5 m cores 1090–1100 mbsf		1.6	
			Log: triple combo, FMS/sonic, magnetometer, UBI			2.5
			Vertical seismic profile **Subtotal = 36.0 days**			0.5
			Hole B: RCB 4.5 m cores 0 to ~26 mbsf **Subtotal = 1.6 days**		1.6	
Ponta Delgada, Azores			Sea voyage from Site AMFW-01A to Ponta Delgada, 936 nmi @ 10.5 kt	3.7		
			Subtotal:	**7.4**	**37.6**	**3.0**
			Total days:		**48.0**	
Alternate sites						
AMFW-01A	~30.17°N, ~42.12°W	1630	HRRS hammer drill-in 22 m of 13 3/8 inch casing		1.9	
			Underream 14 3/4 inch hole with bicenter bit to ~130 mbsf		3.1	
			Run 120 m of 10 3/4 inch casing with MM and underreamer		1.7	
			Run retainer, cement 10 3/4 inch casing		0.9	
			Clean out cement, RCB 130–250 mbsf		3.8	
			RCB 250–370 mbsf		3.8	
			RCB 370–490 mbsf		3.8	
			RCB 490–610 mbsf		3.9	
			RCB 610–730 mbsf		4.0	
			RCB 730–850 mbsf **Subtotal = 31.0 days**		4.1	
			Drop bit; log: triple combo, FMS/sonic, magnetometer, UBI			2.5
			Vertical seismic profile **Subtotal = 3.0 days**			0.5
Footwall peridotite	~30.17°N, ~42.12°W	1630	RCB to bit destruction **Subtotal = 3–5 days**		3–5	
Footwall peridotite	~30.17°N, ~42.12°W	1630	MDCB core ± eight hole transect 0–4.5 mbsf **Subtotal = 1.8 days**		1.8	
AMHW-01A	~30.19°N, ~42.07°W	2580	RAB to bit destruction **Subtotal = 3.0 days**		3.0	
			See additional alternate sites in Table T1.			

Note: RCB = rotary core barrel, FMS = Formation MicroScanner, UBI = ultrasonic borehole imager, HRRS = hard rock reentry system, MM = mud motor, MDCB = motor-driven core barrel, RAB = resistivity at the bit.

Figure F1. Perspective view of Atlantis Massif morphology (vertical exaggeration = ~1.8). Structural components of the Oceanic Core Complex are labeled. Swath bathymetry provides 100% coverage in this area, which extends ~25 km parallel to the spreading axis and ~18 km in the transform direction. Data are gridded at 100 m intervals. RTI = ridge-transform intersection.

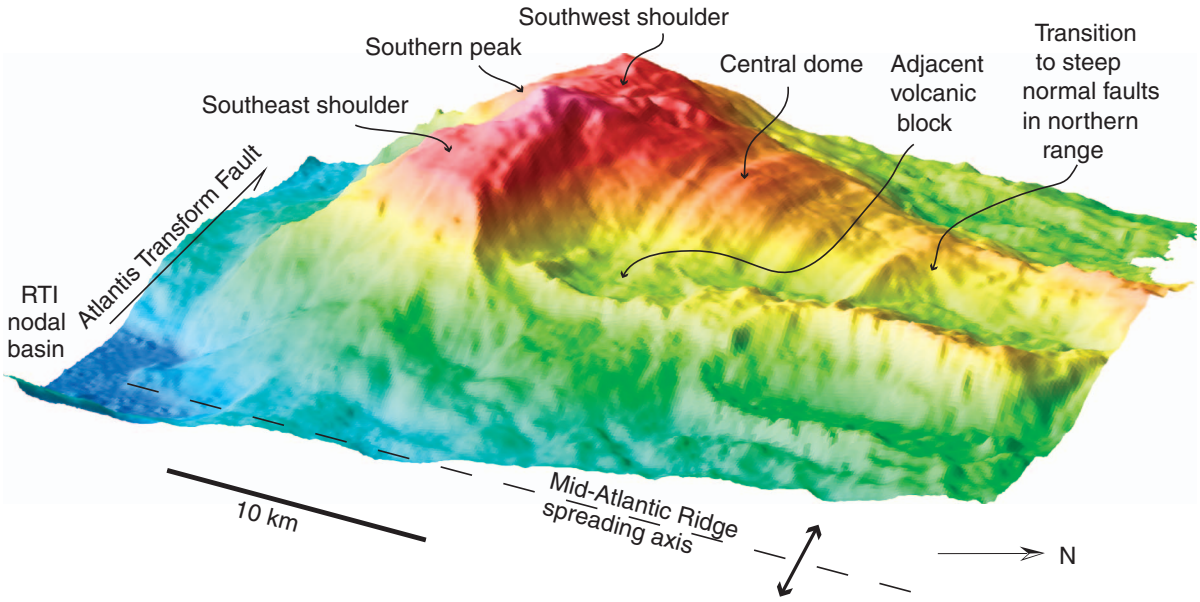

Figure F2. Seismic refraction results. **A.** Map indicating shooting lines and ocean bottom hydrophones (OBH) overlain on bathymetry (m). **B.** NOBEL record section (part of Line 9). Mantle velocities (~8 km/s) are apparent at ranges of 1.6–2 km. **C.** Comparison of subsurface velocity gradients at several seafloor sites. Atlantis Massif gradient is similar to that determined near Site 920, where serpentinized peridotite was recovered. The gradient near Hole 735B, where only gabbro has been recovered, is not as great. MARK = Kane Fracture Zone area, MAR = Mid-Atlantic Ridge, MCS = multichannel seismic, SWIR = Southwest Indian Ridge.

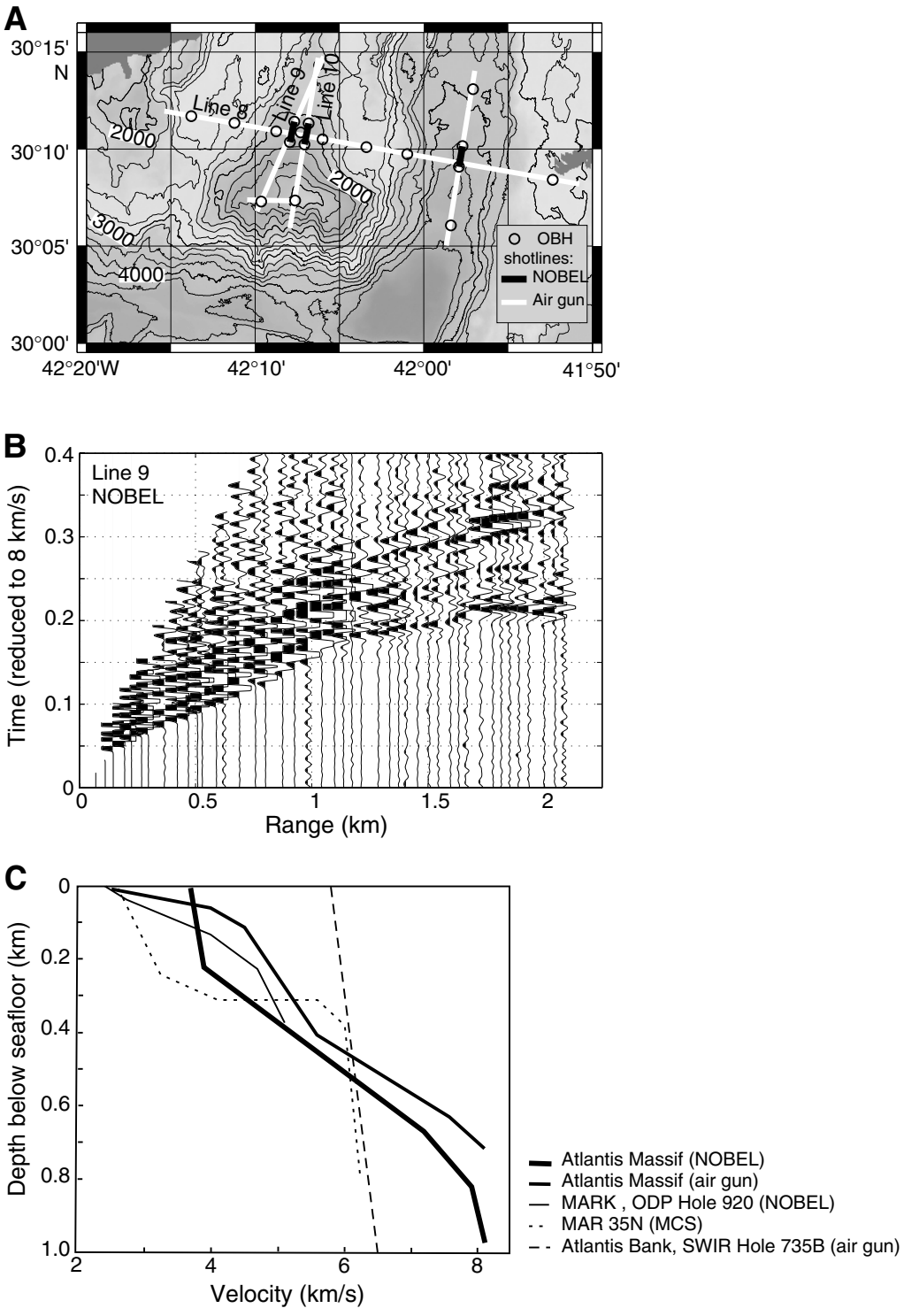

Figure F3. A. Three-dimensional perspective (looking northwest) of the Atlantis Massif (modified from Canales et al., 2004). Circles show IODP drill sites, and location of MCS track lines are indicated (Meg labels). **B.** Common midpoints (CMP) are labeled for reference in subsequent figures. IODP proposed site designations are also labeled for the footwall (AMFW-01A) and hanging wall (AMHW-01A) sites. MCS data were collected by the *Ewing* (EW-0102) in 2001 using a 10-gun array with 3100 in^3 (51 L) capacity. Shot spacing was 37.5 m. The 6 km streamer had 480 channels, and data were sampled every 4 ms. Canales et al. (2004) processed the data by CMP gathers, deconvolution, normal move-out correction, stacking, migration, and dip move-out correction, stacking, migration, and dip move-out filtering.

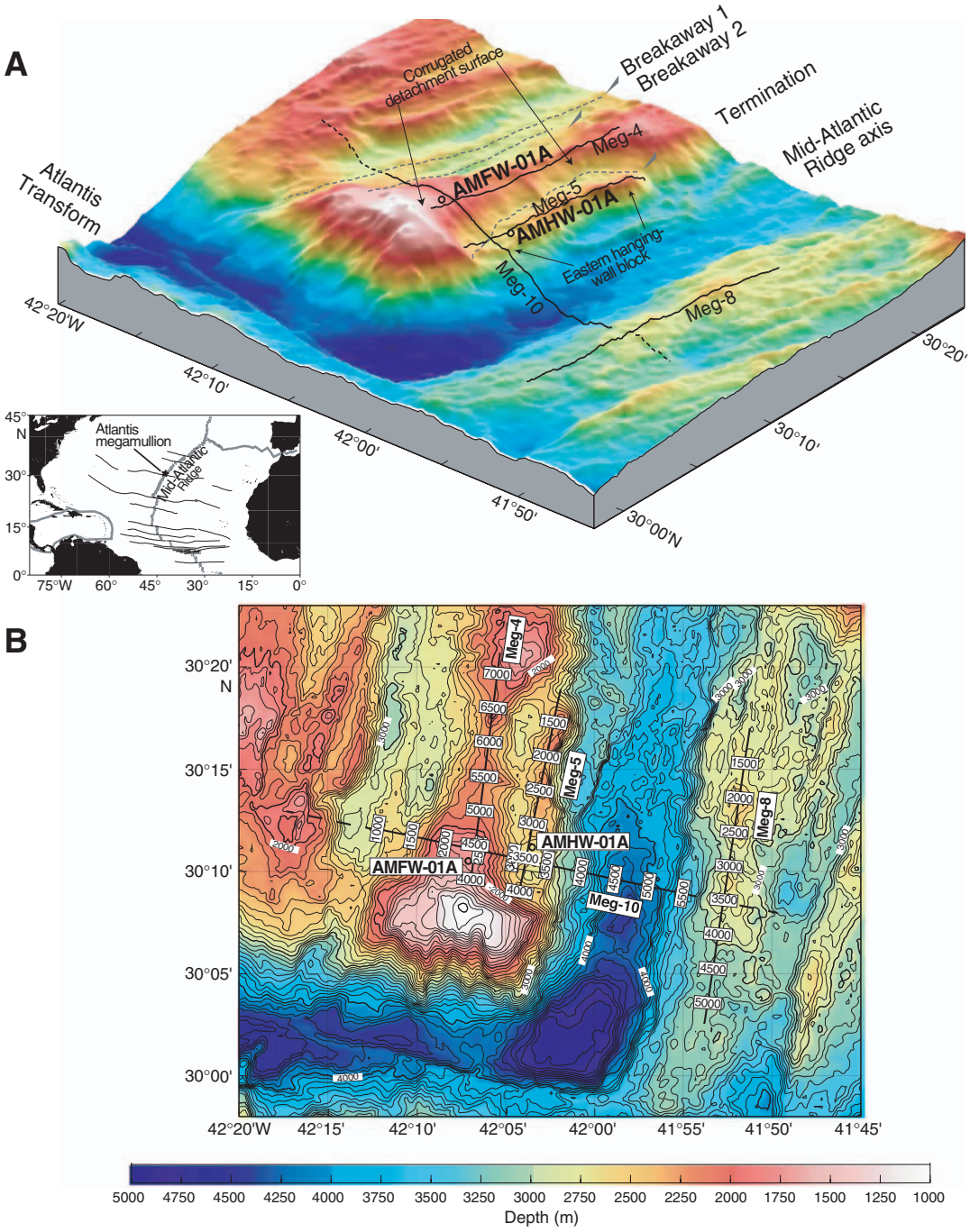

Figure F4. A. Time-migrated MCS line Meg-10 sections modified from Canales et al. (2004) showing the cross-strike structure of the core complex. Reflector D is interpreted to coincide with top of unaltered peridotite. **B.** Gathers for common midpoints (CMPs) 2150–2180 are plotted with move-out correction for 1.5 km/s (left) and 2.25 km/s (right). **C.** Location of Site AMFW-01A is indicated in expanded view of the domal portion of Meg-10. Depth to reflector D (Based on 5 km/s interval velocity determined by Canales et al., 2004) is ~500 m, and total penetration will go as far as possible beyond this. Possible locations for alternate sites are indicated by red arrows (proposed Sites Alt AMFW-02A, 03A, and 04A). As many as three single-bit penetrations might be attempted across the dome along seismic Line Meg-10, between CMPs 1800 and 2600 (exact locations and number of sites to be determined by subsea camera survey, time available for alternate site occupation, and scientific objectives addressed during preceding occupations).

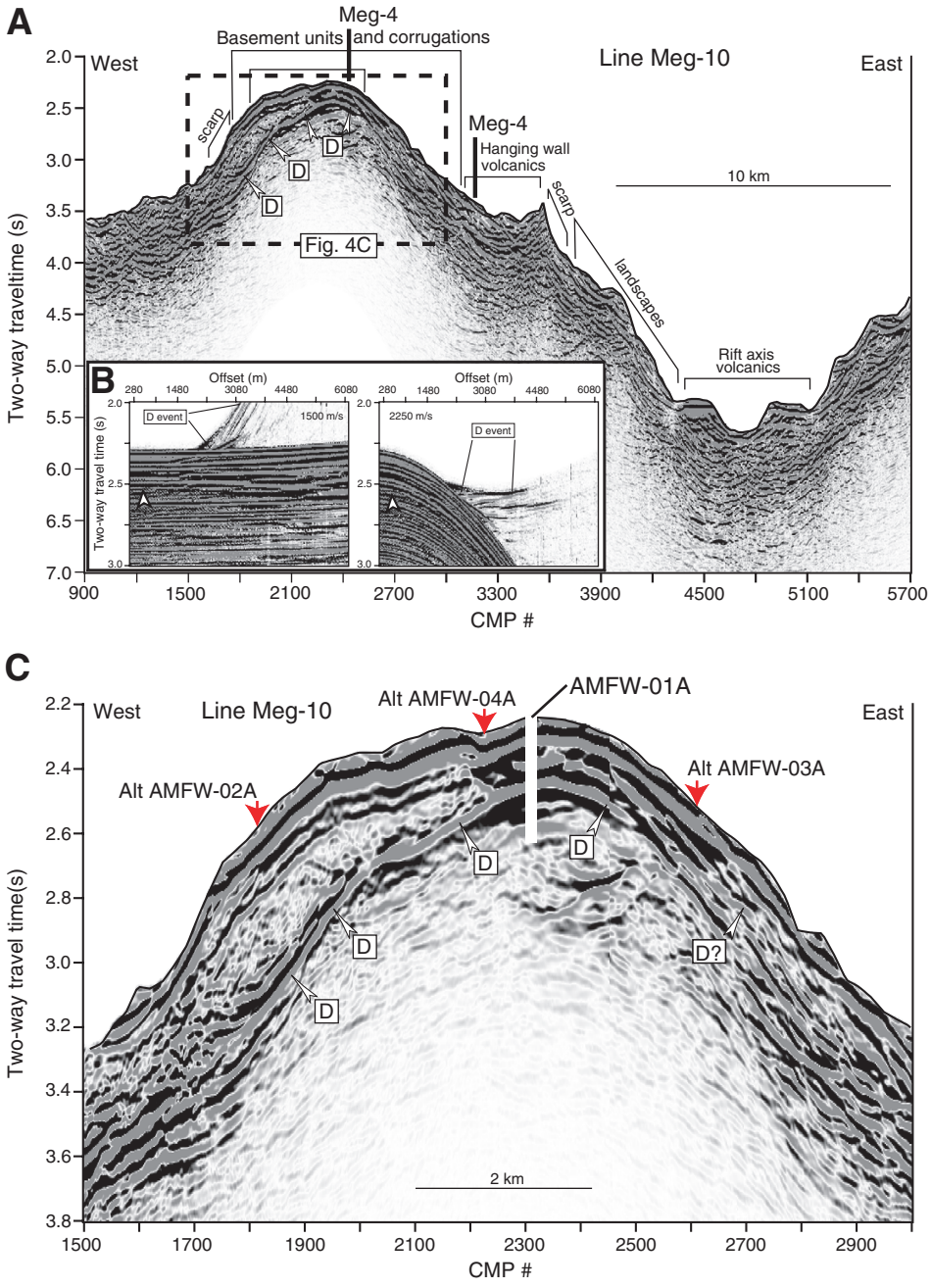

Figure F5. A. Gravity modeling results for profile across the central dome and eastern volcanic block. Residual gravity has contribution of seafloor topography, constant thickness/density crust, and lithospheric cooling removed (Blackman et al., 1998). **B.** Topographic profile shows subsurface blocks of a model that fits the gravity to within the uncertainties of the data.

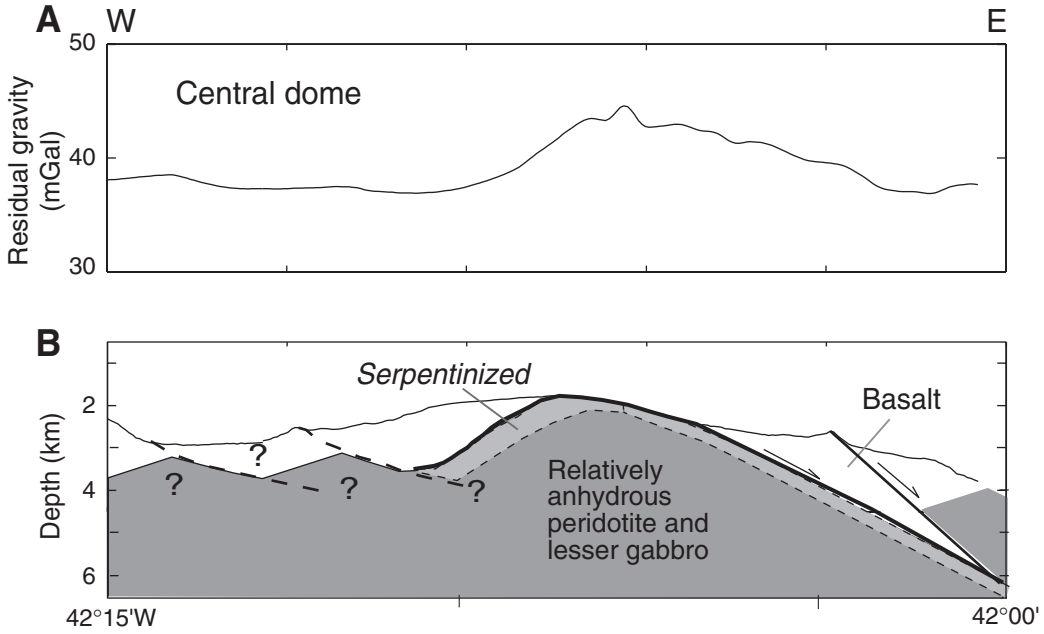

Figure F6. A. Time-migrated MCS line Meg-5, which parallels the strike of the core complex (modified from Canales et al., 2004). Reflector F is interpreted to be the detachment fault where it underlies the hanging wall block. This reflector closely coincides with (**B**) the trace of the exposed detachment when its eastern surface slope is projected at depth to the location of line Meg-5 (yellow line). Location of Site AMHW-01A is indicated. CMP = common midpoint.

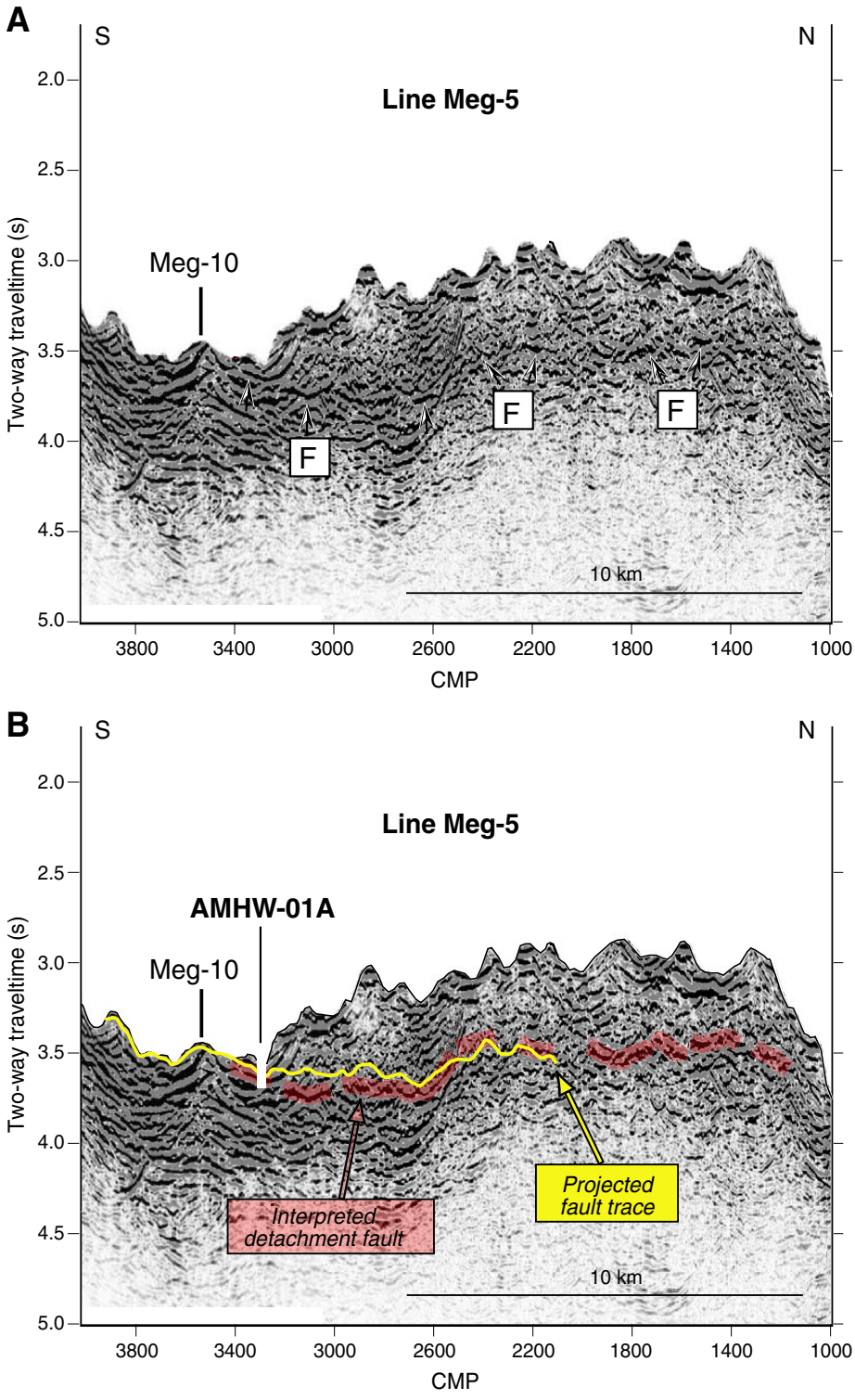

Figure F7. Enlargement of Figure **F3** showing spreading direction–parallel alternate site transect (red solid circles along seismic Line Meg-10), ridge-parallel alternate site transect (green solid circles along seismic Line Meg-4), and southeast shoulder alternate site (blue solid circle on seismic Line Meg-9).

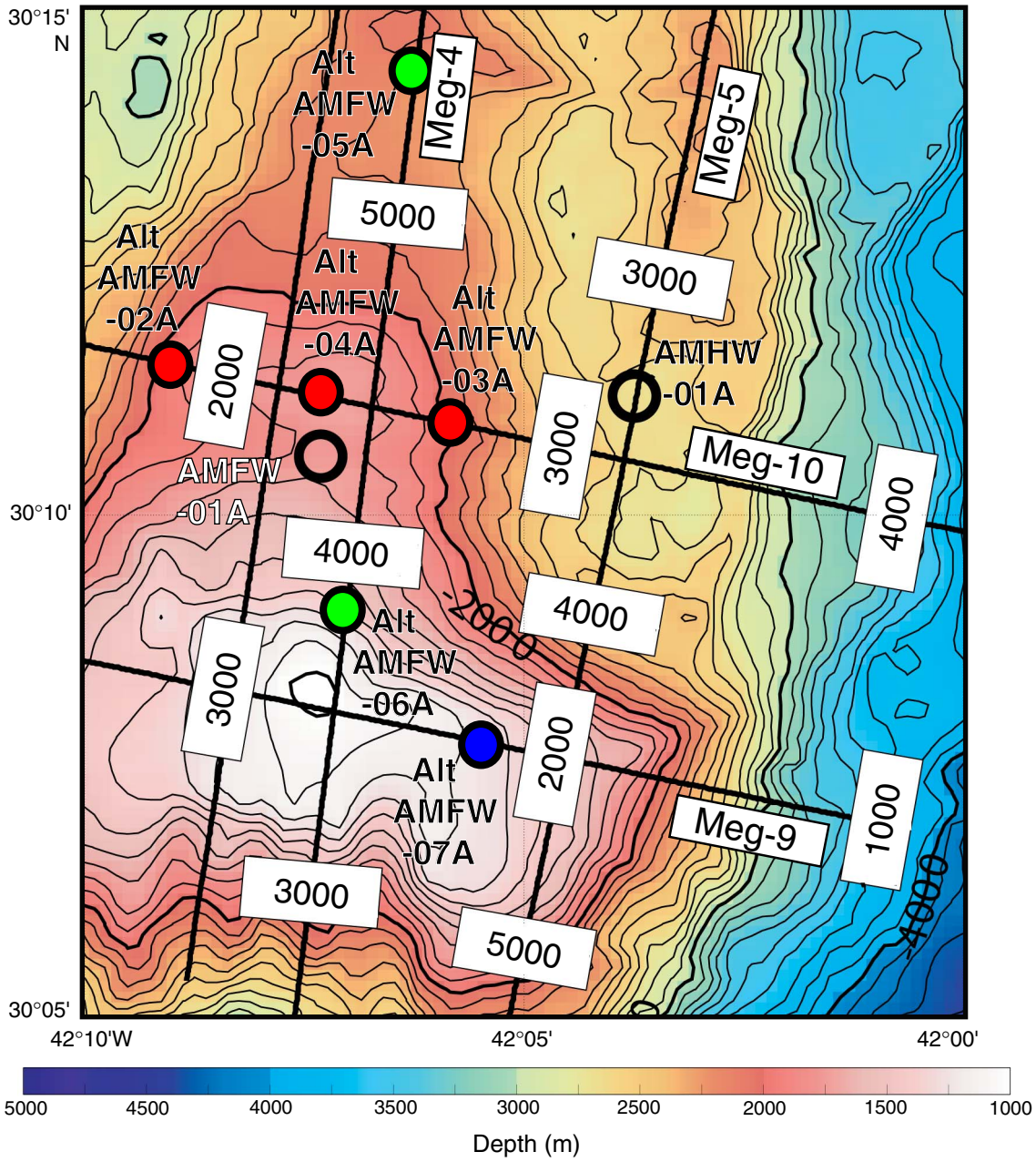

Figure F8. A. Time-migrated MCS Line Meg-4 modified from Canales et al. (2004) showing structure along alternate site ridge-parallel transect (proposed Sites Alt AMFW-05A and 06A). One or two single-bit penetrations might be attempted (depending on time available, previously addressed scientific objectives, and suitable outcrop) between common midpoints (CMPs) 3900 and 5400. Reflector D is interpreted to coincide with top of unaltered peridotite. **B.** Time-migrated MCS Line Meg-9 modified from Canales et al. (2004) showing structure across the dome and the approximate location (between CMPs 2200 and 2400) of an alternate site on the southeast shoulder of the dome (proposed Site Alt AMFW-07A). Reflector D is interpreted to coincide with top of unaltered peridotite.

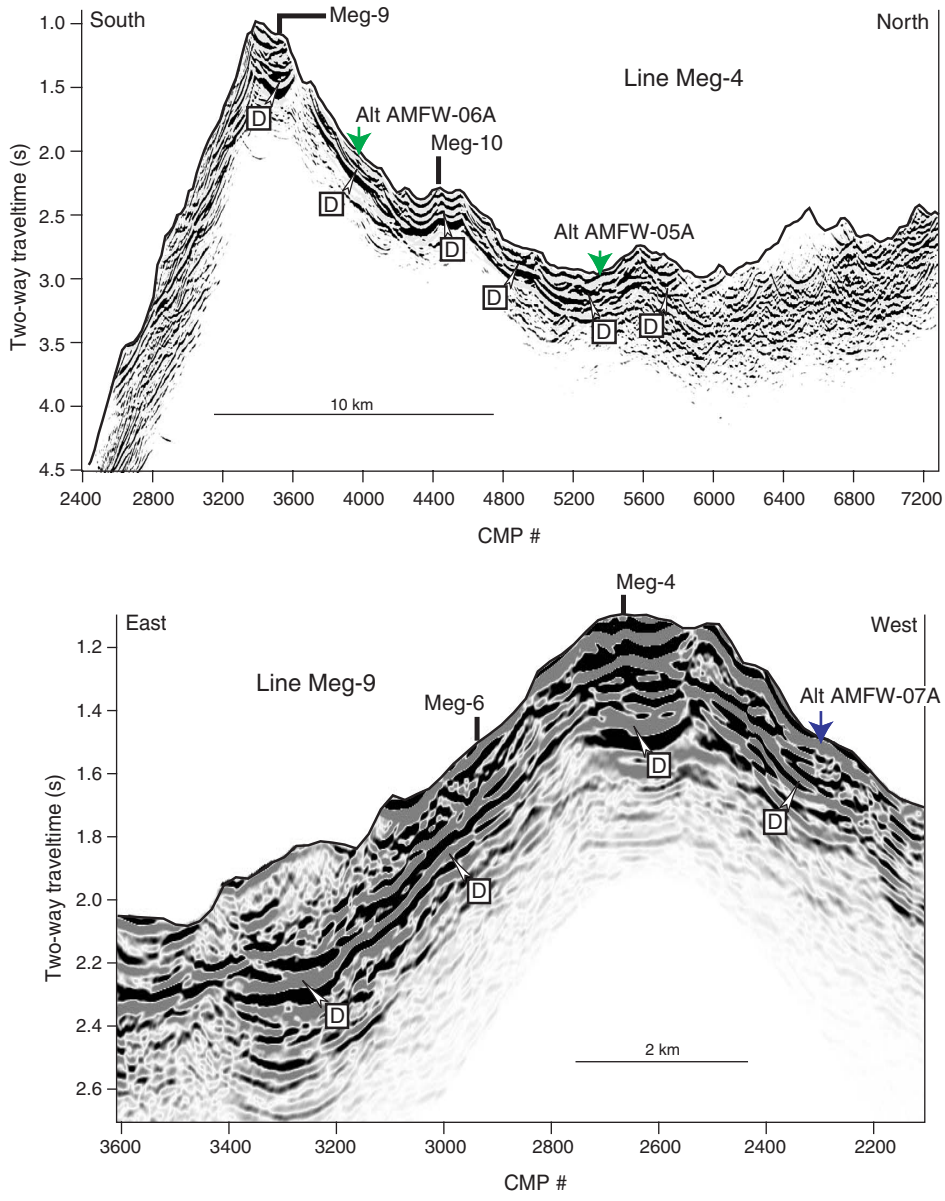

SITE SUMMARIES

Site: AMFW-01A

Priority:	1
Position:	30.17°N, 42.12°W
Water depth (m):	1630
Sediment thickness (m):	1–2
Target drilling depth (mbsf):	>700 into high seismic velocity zone
Approved maximum penetration (mbsf):	700
Survey coverage:	Multichannel seismic data collected by the *Ewing* (EW-0102) in 2001 using a 10-gun array with 3100 in^3 (51 L) capacity. Shot spacing = 37.5 m. The 6 km streamer had 480 channels, and data were sampled every 4 ms. (See Fig. **F4**)
Objectives:	Core through serpentinized peridotite and gabbro into fresh peridotite.
Drilling program:	• Core pilot hole to ±130 mbsf • Log • Install hard rock reentry system to ±20 mbsf in adjacent hole • Drill case to ±130/120 mbsf • Core as deep as possible into fresh peridotite See **"Primary Site: Proposed Site AMFW-01A"**
Logging program:	Five logging runs: • Triple combination tool string • Formation MicroScanner/Dipole Sonic Imager tool string • Ultrasonic Borehole Imager • Borehole magnetometer • Vertical seismic profile
Nature of rock anticipated:	Serpentinized peridotite, gabbro, fresh peridotite

SITE SUMMARIES (CONTINUED)

Site: AMHW-01A

Priority:	1
Position:	30.19°N, 42.06°W
Water depth (m):	2580
Sediment thickness (m):	1–2
Target drilling depth (mbsf):	>400 through detachment fault
Approved maximum penetration (mbsf):	700
Survey coverage:	Multichannel seismic data collected by the *Ewing* (EW-0102) in 2001 using a 10-gun array with 3100 in^3 (51 L) capacity. Shot spacing = 37.5 m. The 6 km streamer had 480 channels, and data were sampled every 4 ms. (See Fig. **F6**)
Objectives:	Core through basalt carapace overlying detachment fault. Continue through fault zone as deep as possible.
Drilling program:	• Install hard rock reentry system to ±20 mbsf • Rotary core to ±70 mbsf • Advanced diamond core to ±130 mbsf • Open hole and install casing to ±120 mbsf • Core as deep as possible through detachment fault See **"Primary Site: Proposed Site AMHW-01A"**
Logging program:	Three logging runs: • Triple combination tool string • Formation MicroScanner/Dipole Sonic Imager tool string • Ultrasonic Borehole Imager
Nature of rock anticipated:	Basalt, fault gouge, serpentinized peridotite, gabbro

SITE SUMMARIES (CONTINUED)

Sites: Alt AMFW-02A, 03A, and 04A

Priority:	Alternate 1
Position:	Along seismic Line Meg-10, endpoints of potential transect at 30.19°N, 42.15°W to 30.18°N, 42.10°W (See Fig. F4)
Water depth (m):	1600–1900
Sediment thickness (m):	1–2
Target drilling depth (mbsf):	Single bit penetration
Approved maximum penetration (mbsf):	
Survey coverage:	Specific sites to be determined by time available and subsea camera survey between common midpoints 1800 and 2600
Objectives:	Transect of spreading direction–parallel sites over the central dome to investigate unroofing rates and age of initial fault exposure
Drilling program:	Single bit to destruction or until objectives reached
Logging program:	Contingent on depth of penetration and hole conditions
Nature of rock anticipated:	Serpentinized peridotite, gabbro

SITE SUMMARIES (CONTINUED)

Sites: Alt AMFW-05A and 06A

Priority:	Alternate 2
Position:	Along seismic Line Meg-4, endpoints of potential transect at 30.15°N, 42.12°W to 30.24°N, 42.11°W (See Fig. **F8**)
Water depth (m):	1600–2200
Sediment thickness (m):	1–2
Target drilling depth (mbsf):	Single bit penetration
Approved maximum penetration (mbsf):	
Survey coverage:	Specific sites to be determined by time available and subsea camera survey between common midpoints 3900 and 5400
Objectives:	Transect of ridge-parallel sites along the central dome to investigate heterogeneity in microstructure, geochemistry, and petrology along the dome moving from the ridge segment end toward its center
Drilling program:	Single bit to destruction or until objectives reached
Logging program:	Contingent upon depth of penetration and hole conditions
Nature of rock anticipated:	Serpentinized peridotite, gabbro

SITE SUMMARIES (CONTINUED)

Site: Alt AMFW-07A

Priority:	Alternate 3
Position:	Along seismic Line Meg-9 at ~30.13°N, ~42.09°W (See Fig. F8)
Water depth (m):	1000–1200
Sediment thickness (m):	1–2
Target drilling depth (mbsf):	Shallow penetration
Approved maximum penetration (mbsf):	
Survey coverage:	Site to be determined by subsea camera survey, between common midpoints 2200 and 2400
Objectives:	Investigate different portions of the detachment fault systems by comparison to other alternate and primary sites
Drilling program:	Single bit to destruction or until objectives reached
Logging program:	Contingent upon depth of penetration and hole conditions
Nature of rock anticipated:	Serpentinized peridotite, gabbro

EXPEDITION 304 SCIENTIFIC PARTICIPANTS*

Barbara E. John
Co-Chief Scientist
Department of Geology and Geophysics
University of Wyoming
1000 East University
PO Box 3006
Laramie WY 82071
USA
bjohn@uwyo.edu
Work: (307) 766-4232
Fax: (307) 766-6679

Donna Blackman
Co-Chief Scientist
Scripps Institution of Oceanography
University of California, San Diego
9500 Gilman Drive
La Jolla CA 92093-0225
USA
dblackman@ucsd.edu
Work: (858) 534-8813
Fax: (858) 534-5332

D. Jay Miller
Staff Scientist
Integrated Ocean Drilling Program
Texas A&M University
1000 Discovery Drive
College Station TX 77845-9547
USA

Eric S. Andal
Igneous Petrologist
Department of Earth Sciences
Kanazawa University
Kakumamachi
Kanazawa, Ishikawa 920-1192
Japan
andal_es@earth.s.kanazawa-u.ac.jp
Work: (81) 076-264-5726
Fax: (81) 076-264-5746

Muriel Andreani
Metamorphic Petrologist
Laboratoire de Geosciences Marines–
CNRS UMR 7097
Institut de Physique du Globe de Paris
75252 Paris Cedex
France
Muriel.Andreani@obs.ujf-grenoble.fr
Work: (33) 1-44-27-5193

Florence Einaudi
Laboratoire de Mesures en Forage
ODP/Naturalia et Biologia (NEB)
BP 72
13545 Aix-en-Provence Cedex 4
France
einaudi@lmf-aix.gulliver.fr
Work: (33) 4 67 14 93 09
Fax: (33) 4 67 14 93 08

Bryce R. Frost
Metamorphic Petrologist
Department of Geology and Geophysics
University of Wyoming
1000 East University Avenue
Department 3006
Laramie WY 82071
USA
rfrost@uwyo.edu
Work: (307) 766-4290
Fax: (307) 766-6679

Marion Drouin
Metamorphic Petrologist
Laboratoire de Tectonophysique
Université Montpellier II
Montpellier Cedex 34095
France
marion.drouin@dstu.univ-montp2.fr
Work: (33) 4-72-43-1479
Fax: (33) 4-72-44-8382

Jeffrey S. Gee
Paleomagnetist
Geosciences Research Division
Scripps Institution of Oceanography
University of California, San Diego
Mail code 0220
La Jolla CA 92093-0220
USA
jsgee@ucsd.edu
Work: (858) 534-4707
Fax: (858) 534-0784

*At time of publication; subject to change.

Marguerite M. Godard
Geochemist
Laboratoire de Tectonophysique
Université Montpellier II
Case Courrier 49
Place Eugéne Bataillon
34095 Montpellier Cedex 5
France
margot@dstu.univ-montp2.fr
Work: (33) 467-14-39-37
Fax: (33) 467-14-36-03

Nicholas W. Hayman
Structural Geologist
Division of Earth and Ocean Sciences
Duke University
103 Old Chemistry Building
Durham NC 27708-0230
USA
hayman@duke.edu
Work: (919) 681-8165
Fax: (919) 684-5833

Takehiro Hirose
Structural Geologist
Geologisches Institut
Eidgenössische Technische Hochschule–Zentrum
Sonneggstrasse 5, NOH34-4
8092 Zürich
Switzerland
hirose@erdw.ethz.ch
Work: (41) 1-632-3636
Fax: (41) 1-632-1080

Andrew M. McCaig
Metamorphic Petrologist/Structural Geologist
School of Earth Sciences
University of Leeds
Leeds LS2 9JT
United Kingdom
andrew@earth.leeds.ac.uk
Work: (44) 113-3435219
Fax: (44) 113-3435259

Antony Morris
Paleomagnetist
School of Earth, Ocean, and Environmental Sciences
University of Plymouth
Drake Circus
Plymouth PL4 8AA
United Kingdom
amorris@plymouth.ac.uk
Work: (44) 1752-233120
Fax: (44) 1752-233117

Tatsunori Nakagawa
Microbiologist
Graduate School of Science
Department of Mineralogy, Petrology, and Economic Geology
Tohoku University
Aoba, Aramaki-Aza, Aoba-ku
Sendai, Miyagi 980-8578
Japan
n-takko@ganko.tohoku.ac.jp
Work: (81) 22-217-6660
Fax: (81) 22-217-6634

Roger C. Searle
Physical Properties Specialist
Department of Earth Sciences
University of Durham
South Road
Durham, County Durham DH1 3LE
United Kingdom
r.c.searle@durham.ac.uk
Work: (44) 191-334-2307
Fax: (44) 191-334-2301

Anette von der Handt
Igneous Petrologist
Abeilung Geochemie
Max-Planck-Institüt für Chemie
PO Box 3060
55020 Mainz
Germany
avdhandt@mpch-mainz.mpg.de
Work: (49) 6131-3055301
Fax: (49) 6131-371051

Michael A. Storms
Operations Superintendent
Integrated Ocean Drilling Program
Texas A&M University
1000 Discovery Drive
College Station TX 77845-9547
USA
storms@iodp.tamu.edu
Work: (979) 845-2101
Fax: (979) 845-2308

Burnette W. Hamlin
Laboratory Officer
Integrated Ocean Drilling Program
Texas A&M University
1000 Discovery Drive
College Station TX 77845-9547
USA
hamlin@iodp.tamu.edu
Work: (979) 845-2496
Fax: (979) 845-0876

Timothy Bronk
Assistant Laboratory Officer
Integrated Ocean Drilling Program
Texas A&M University
1000 Discovery Drive
College Station TX 77845-9547
USA
bronk@iodp.tamu.edu
Work: (979) 845-0879
Fax: (979) 845-0876

William Crawford
Imaging Specialist
Integrated Ocean Drilling Program
Texas A&M University
1000 Discovery Drive
College Station TX 77845-9547
USA
crawford@iodp.tamu.edu
Work: (979) 862-7757
Fax: (979) 458-1617

Christopher Bennight
Marine Laboratory Specialist: Chemistry
Integrated Ocean Drilling Program
Texas A&M University
1000 Discovery Drive
College Station TX 77845-9547
USA
bennight@iodp.tamu.edu
Work: (979) 458-1874
Fax: (979) 845-2308

Lisa Brandt
Marine Laboratory Specialist: Chemistry
Ocean Drilling Program
Texas A&M University
1000 Discovery Drive
College Station TX 77845-9547
USA
brandt@iodp.tamu.edu
Work: (979) 845-3602
Fax: (979) 845-0876

Jason Deardorff
Marine Laboratory Specialist: X-Ray
Integrated Ocean Drilling Program
Texas A&M University
1000 Discovery Drive
College Station TX 77845-9547
USA
deardorff@iodp.tamu.edu
Work: (979) 845-9186
Fax: (979) 845-2308

Peter Kannberg
Marine Laboratory Specialist:
Downhole Tools, Thin Sections
Integrated Ocean Drilling Program
Texas A&M University
1000 Discovery Drive
College Station TX 77845-9547
USA
pk001i@hotmail.com

Heather Paul
Marine Laboratory Specialist: Physical Properties
Integrated Ocean Drilling Program
Texas A&M University
1000 Discovery Drive
College Station TX 77845-9547
USA
hjpaul@uvic.ca

Paul Teniere
Assistant Laboratory Officer/MLS: Paleomagnetism
Integrated Ocean Drilling Program
Texas A&M University
1000 Discovery Drive
College Station TX 77845-9547
USA
teniere@hotmail.com

Randy W. Gjesvold
Marine Instrumentation Specialist
Integrated Ocean Drilling Program
Texas A&M University
1000 Discovery Drive
College Station TX 77845-9547
USA
gjesvold@iodp.tamu.edu
Work: (979) 845-3602
Fax: (979) 845-0876

Michael Meiring
Marine Instrumentation Specialist
Integrated Ocean Drilling Program
Texas A&M University
1000 Discovery Drive
College Station TX 77845-9547
USA
kleinmeiring@yahoo.com
Work: (979) 845-3602
Fax: (979) 845-0876

Margaret Hastedt
Marine Computer Specialist
Integrated Ocean Drilling Program
Texas A&M University
1000 Discovery Drive
College Station TX 77845-9547
USA
hastedt@iodp.tamu.edu
Work: (979) 862-2315
Fax: (979) 458-1617

David Morley
Marine Computer Specialist
Integrated Ocean Drilling Program
Texas A&M University
1000 Discovery Drive
College Station TX 77845-9547
USA
morley@iodp.tamu.edu
Work: (979) 862-4847
Fax: (979) 845-4857

Deepak Kannoju
Programmer Specialist
Integrated Ocean Drilling Program
Texas A&M University
1000 Discovery Drive
College Station TX 77845-9547
USA
kannoju@iodp.tamu.edu
Work: (979) 845-6635
Fax: (979) 458-1617

Jennifer Henderson
Marine Laboratory Specialist: Core
Integrated Ocean Drilling Program
Texas A&M University
1000 Discovery Drive
College Station TX 77845-9547
USA
henderson@iodp.tamu.edu
Work: (979) 874-6572
Fax: (979) 874-6837

Karen Johnston
Marine Laboratory Specialist: Underway Geophysics
Integrated Ocean Drilling Program
Texas A&M University
1000 Discovery Drive
College Station TX 77845-9547
USA
johnston@iodp.tamu.edu
Work: (979) 845-3602
Fax: (979) 845

EXPEDITION 305 SCIENTIFIC PARTICIPANTS*

Benoit Ildefonse
Co-Chief Scientist
Laboratoire de Tectonophysique
Universite Montpellier II
Universite Montpellier 2, CC49
34095 Montpellier
France
benoit@dstu.univ-montp2.fr
Work: (33) 46714-3818
Fax: (33) 46714-3603

Yasuhiko Ohara
Co-Chief Scientist
Ocean Research Laboratory
Hydrographic and Oceanographic Department of Japan
5-3-1 Tsukiji, Chuo-ku
Tokyo 104-0045
Japan
ohara@jodc.go.jp
Work: (81) 3-3541-4387
Fax: (81) 3-3541-3870

D. Jay Miller
Staff Scientist/Expedition Project Manager
Integrated Ocean Drilling Program
Texas A&M University
1000 Discovery Drive
College Station TX 77845-9547
USA
miller@iodp.tamu.edu
Work: (979) 845-2197
Fax: (979) 845-0876

Natsue Abe
Igneous Petrologist
Deep Sea Research Department
Japan Marine Science and Technology Center
2-15 Natsushima-cho
Yokosuka, Kanagawa 237-0061
Japan
abenatsu@jamstec.go.jp
Work: (81) 46-867-9329
Fax: (81) 46-867-9315

Donna Blackman
Physical Properties Specialist
See Expedition 304 list for contact information

James S. Beard
Metamorphic Petrologist
Department of Earth Sciences
Virginia Museum of Natural History
1001 Douglas Avenue
Martinsville VA 24112
USA
jbeard@vmnh.net
Work: (276) 666-8611
Fax: (276) 632-6487

Daniele Brunelli
Igneous Petrologist
Laboratoire Pierre Süe–DRECAM
CNRS
91191 Yvette Cedex
France
brunelli@drecam.cea.fr
Work: (33) 1-6908-9522
Fax: (33) 1-6908-6923

Heike Delius
Logging Staff Scientist
Department of Geology
University of Leicester
University Road
Leicester LE1 7RH
United Kingdom
hd21@le.ac.uk
Phone: (44) 116-252-3634
Fax: (44) 116-252-3918

Javier Escartin
Structural Geologist
Marine Geosciences
Université Pierre et Marie Curie
Case 89 IPGP
4 Place Jussieu
75252 Paris
France
escartin@ipgp.jussieu.fr
Work: (33) 1-4427-4601
Fax: (33) 1-4427-9969

Patricia B. Fryer
Metamorphic Petrologist
School of Ocean and Earth Science and Technology
University of Hawaii at Manoa
1680 East-West Road
Honolulu HI 96822
USA
pfryer@hawaii.edu
Work: (808) 956-3146
Fax: (808) 956-6322

*At time of publication; subject to change.

Akihiro Tamura Hasebe
Igneous Petrologist
Department of Earth Sciences
Kanazawa University
Kakuma, Kanazawa 920-1192
Japan
kamui@kenroku.kanazawa-u.ac.jp
Work: (81) 76-264-5723
Fax: (81) 76-264-5746

Eric Hellebrand
Igneous Petrologist
Abteilung Geochemie
Max-Planck-Institüt für Chemie
Postfach 3060
55020 Mainz
Germany
ehelle@mpch.mainz.mpg.de
Work: (49) 6131-305220
Fax: (49) 6131-371051

Benoit Ildefonse
(See Co-chief information above)

Satoko Ishimaru
Geochemist
Division of Environmental Science and Engineering
Kanazawa University
Graduate School of Natural Science and Technology
Kakuma, Kanazawa 920-1192
Japan
jaja@earth.s.kanazawa-u.ac.jp
Work: (81) 76-264-5723
Fax: (81) 76-264-5746

Kevin T.M. Johnson
Igneous Petrologist
Department of Geology and Geophysics/SOEST
University of Hawaii and Manoa
1680 East-West Road
Post 606B
Honolulu HI 96822
USA
kjohnso2@hawaii.edu
Work: (808) 956-3444
Fax: (808) 956-5512

Katsuyoshi Michibayashi
Structural Geologist
Institute of Geosciences
Shizuoka University
Faculty of Science
836 Oya
Shizuoka 422-8529
Japan
sekmich@ipc.shizuoka.ac.jp
Work: (81) 54-238-4788
Fax: (81) 54-238-0491

Toshio Nozaka
Metamorphic Petrologist
Department of Earth Sciences
Okayama University
3-1-1 Tsushima-naka
Okayama 700-8530
Japan
nozaka@cc.okayama-u.ac.jp
Work: (81) 86-251-7883
Fax: (81) 86-251-7895

Guenter Suhr
Structural Geologist
Mineralogisch-Petrographisches Institut
Universität Köln
Zülpicher Strasse 49b
50674 Köln
Germany
suhr@min.uni-koeln.de
Work: (49) 221-470-3196
Fax: (40) 221-470-5199

Ronald M. Grout
Operations Superintendent
Integrated Ocean Drilling Program
Texas A&M University
1000 Discovery Drive
College Station TX 77845-9547
USA
grout@iodp.tamu.edu
Work: (979) 845-2144
Fax: (979) 845-2308

Roy Davis
Laboratory Officer
Integrated Ocean Drilling Program
Texas A&M University
1000 Discovery Drive
College Station TX 77845-9547
USA
davis@iodp.tamu.edu
Work: (979) 845-2367
Fax: (979) 845-0876

Chieh Peng
Assistant Laboratory Officer
Integrated Ocean Drilling Program
Texas A&M University
1000 Discovery Drive
College Station TX 77845-9547
USA
peng@iodp.tamu.edu
Work: (979) 845-0879
Fax: (979) 845-0876

Margo Cortes
Yeoperson
Joint Oceanographic Institutions, Inc.
1201 New York Avenue, NW, Suite 400
Washington, DC 20005
USA
mcortes@joiscience.org
Work: (202) 232-3900 ext. 1618

Trevor J. Cobine
Marine Laboratory Specialist: Paleomagnetism
Integrated Ocean Drilling Program
Texas A&M University
1000 Discovery Drive
College Station TX 77845-9547
USA
tcobine@metz.une.edu.au
Work: (61) 02-6773-2860
Fax: (61) 02-6773-3300

Lisa K. Crowder
Assistant Laboratory Officer/
MLS: Underway Geophysics
Integrated Ocean Drilling Program
Texas A&M University
1000 Discovery Drive
College Station TX 77845-9547
USA
crowder@iodp.tamu.edu
Work: (979) 845-7716
Fax: (979) 845-0876

Dennis Graham
Marine Laboratory Specialist: Chemistry
Integrated Ocean Drilling Program
Texas A&M University
1000 Discovery Drive
College Station TX 77845-9547
USA
graham@iodp.tamu.edu
Work: (979) 845-3602
Fax: (979) 845-0876

Charlie Endris
Marine Laboratory Specialist:
Downhole Tools, Thin Sections
Integrated Ocean Drilling Program
Texas A&M University
1000 Discovery Drive
College Station TX 77845-9547
USA

Michael J. Hodge
Marine Computer Specialist
Integrated Ocean Drilling Program
Texas A&M University
1000 Discovery Drive
College Station TX 77845-9547
USA
hodge@iodp.tamu.edu
Work: (979) 862-4845
Fax: (979) 458-1617

Leah Shannon Housley
Imaging Specialist
Integrated Ocean Drilling Program
Texas A&M University
1000 Discovery Drive
College Station TX 77845-9547
USA
housley@iodp.tamu.edu
Work: (979) 862-7757
Fax: (979) 458-1617

Eric Jackson
Marine Laboratory Specialist: X-Ray
Integrated Ocean Drilling Program
Texas A&M University
1000 Discovery Drive
College Station TX 77845-9547
USA
geocrust@yahoo.com
Work: (979) 845-3602
Fax: (979) 845-0876

Jan Jurie Kotze
Marine Instrumentation Specialist
Integrated Ocean Drilling Program
Texas A&M University
1000 Discovery Drive
College Station TX 77845-9547
USA
kotzejj@megaweb.co.za
Work: (979) 845-3602
Fax: (979) 845-0876

Erik Moortgat
Marine Computer Specialist
Integrated Ocean Drilling Program
Texas A&M University
1000 Discovery Drive
College Station TX 77845-9547
USA
moortgat@iodp.tamu.edu
Work: (979) 458-1615
Fax: (979) 458-1617

Pieter Pretorius
Marine Instrumentation Specialist
Integrated Ocean Drilling Program
Texas A&M University
1000 Discovery Drive
College Station TX 77845-9547
USA
pretorius@iodp.tamu.edu
Work: (979) 845-3602
Fax: (979) 845-0876

Yasmin Yabyabin
Marine Laboratory Specialist: Underway Geophysics
Integrated Ocean Drilling Program
Texas A&M University
1000 Discovery Drive
College Station TX 77845-9547
USA
yas@ldeo.columbia.edu
Work: (845) 365-8630

Paula Weiss
Curator
Integrated Ocean Drilling Program
Texas A&M University
1000 Discovery Drive
College Station TX 77845-9547
USA
pweiss@qwest.net
Work: (979) 845-3602
Fax: (979) 845-0876

Robert M. Wheatley
Marine Laboratory Specialist: Chemistry
Integrated Ocean Drilling Program
Texas A&M University
1000 Discovery Drive
College Station TX 77845-9547
USA
wheatley@iodp.tamu.edu
Work: (979) 458-1067
Fax: (979) 845-0876

Lena Maeda
Marine Laboratory Specialist: Core
Integrated Ocean Drilling Program
Texas A&M University
1000 Discovery Drive
College Station TX 77845-9547
USA

Michael Murphy
Marine Laboratory Specialist: Physical Properties
Integrated Ocean Drilling Program
Texas A&M University
1000 Discovery Drive
College Station TX 77845-9547
USA